

In vitro and in silico antiviral activity of di-halogenated compounds derived from L-tyrosine against human immunodeficiency virus 1 (HIV-1).

MARIA SULENY SERNA ARBELAEZ

Research work submitted in fulfillment of the requirements for the degree of Master in Basic Biomedical Science, emphasis in Virology

ADVISOR

Wildeman Zapata Builes, Bact., MSc., DSc.

CO-ADVISOR

Elkin Galeano, Q.F., MSc., DSc.

ADVISORY COMMITTEE

Juan Carlos Hernández, Microbiol., DSc.

Jaime Andrés Pereañez, Q.F., DSc.

Juan Carlos Quintana, Bact., MSc., DSc.

Universidad de Antioquia

Corporación Académica Ciencias Básicas Biomédicas

Medellín, Colombia

2022

Este trabajo está dedicado con cariño a mi familia; especialmente a mis padres, que han sido mi apoyo a lo largo de mi carrera universitaria y de mi vida. Ellos han depositado su confianza en mí para lograr una meta más en mi vida.

Agradecimientos

A mi familia por su paciencia y amor incondicional en este proceso.

A mi asesor, el profesor Wildeman Zapata por permitirme participar en este proyecto, por sus consejos, apoyo y paciencia al enseñarme todo lo que me permitió realizar este trabajo.

A los miembros del comité asesor por sus consejos y aportes para la realización del trabajo.

A los grupos de investigación INFETTARE, inmunodeficiencias primarias, e inmunovirología por abrirme sus puertas y permitirme crecer personal y profesionalmente.

A todos mis compañeros del grupo de Inmunodeficiencias primarias y de inmunovirología, especialmente a Julián Rojas, Diana Arboleda y Daniel Rincón por su ayuda, generosidad y apoyo incondicional.

No podría haber completado mi trabajo de tesis sin el apoyo de mis amigos, ya que siempre han sido un apoyo emocional incluso en los momentos más difíciles.

TABLE OF CONTENTS

RESUMEN	6
ABSTRACT	7
INTRODUCTION	11
General aspects of the HIV-1 infection	12
HIV-1 replication steps	13
HIV therapy targets and agents	13
Viral entry Inhibitors	14
Attachment Inhibitors.....	14
Co-receptor antagonists.....	14
Fusion Inhibitors	15
Reverse transcriptase inhibitors	15
Nucleoside/Nucleotide RT Inhibitors (NRTIs).....	15
Nucleoside RT Inhibitors (NNRTIs).....	16
Integrase strand transferase inhibitors (INSTIs).....	16
Inhibitors of the Viral Maturation - Protease inhibitors (PIs).....	16
Natural compounds and derivatives with antiviral activity against HIV	17
OBJECTIVES.....	19
General objective	19
Specific objectives	19
RESEARCH QUESTION	19
HYPOTHESIS.....	19
MATERIALS AND METHODS	19
Di-halogenated compounds derived from L-Tyrosine.....	19
Cell maintenance.....	23
Production of viral stocks	24
Quantification of p24 by ELISA.....	25
Determination of cytotoxicity.....	25
Antiviral screening.....	26
VSV-pseudotyped HIV-1 Infection Assay and quantification of viral particles: Flow cytometry.	27
Evaluation of the interaction of compounds with viral proteins by molecular docking... Ligand preparation	27

Protein preparation	27
<i>In silico</i> toxicological modeling	29
Statistical analysis.....	30
RESULTS.....	30
Di-halogenated compounds derived from L-tyrosine have no significant cytotoxic effect on TZM-bl cells.	30
Di-halogenated compounds showed low <i>in silico</i> toxicity.	33
Anti-HIV-1 BaL (R5 strain) <i>in vitro</i> activity screening of di-halogenated compounds...	37
Anti- HIV-1 _{IIIB} (X4 strain) <i>in vitro</i> activity screening of di-halogenated compounds	43
Table 8. Selectivity index of the compounds against HIV-1 _{IIIB}	48
Anti-HIV-GFP-VSV-G <i>in vitro</i> activity of di-halogenated compounds.....	48
The L-tyrosine derivatives exhibit favorable binding energies with the tested proteins. .	52
DISCUSSION.....	63
CONCLUSION	69
LIMITATIONS AND PERSPECTIVES OF THE STUDY	69
ADDITIONAL INFORMATION	71
REFERENCES	74
SUPPLEMENTARY INFORMATION.....	80

RESUMEN

Introducción: la infección por el VIH-1 se considera uno de los principales problemas de salud pública en todo el mundo. Debido al limitado acceso a la terapia antirretroviral, a los efectos secundarios asociados y a la resistencia que puede generar el virus, se ha hecho necesario continuar con el desarrollo de nuevos agentes antivirales. Los productos naturales y sus derivados han mostrado potencial terapéutico contra el VIH-1, entre estos se incluyen la zidovudina, el bevirimat, el calanolide A, entre otros. En el presente estudio se propuso identificar el potencial anti-VIH-1 (*in vitro* e *in silico*) de dieciséis compuestos sintéticos dihalogenados derivados de la L-Tirosina.

Metodología: la modelación toxicológica se realizó con ADMET Predictor® y el acoplamiento molecular con proteínas virales fue evaluado *in silico* usando Autodock Vina®. La citotoxicidad *in vitro* fue determinada por MTT en la línea celular TZM-bl. Se realizó una estrategia de tamizaje antiviral combinada (tratamiento pre y post infección) en células TZM-bl, infectadas con VIH-1 (cepas R5 y X4). El efecto inhibitorio fue cuantificado mediante la actividad de la luciferasa. Por otra parte, se determinó la actividad antiviral de los compuestos más promisorios frente a un virus pseudotipado (HIV-GFP-VSV-G) mediante citometría de flujo.

Resultados: se observó una menor toxicidad *in silico* e *in vitro* de los compuestos derivados de las L-tirosinas con el OH libre comparado con los compuestos derivados de la tiramina. Los compuestos TODB-2M, TODC-2M, TODC-3M y YDC-3M demostraron una actividad inhibitoria estadísticamente significativa mayor al 40% frente a las cepas X4 y R5 del VIH-1, y mayor al 12% contra el virus HIV-GFP-VSV-G. Finalmente, los resultados *in silico* mostraron una energía de unión favorable, principalmente con la proteasa, la transcriptasa reversa o la gp120.

Conclusión: los compuestos TODB-2M, TODC-2M, TODC-3M y YDC-3M tienen potencial antiviral frente al VIH-1. La actividad antiviral, puede deberse a la interacción con la transcriptasa inversa y/o la proteasa viral, o con la gp120 de la envoltura.

Palabras clave: VIH-1, antiviral, citotoxicidad, acoplamiento molecular, derivados de L-tirosina.

ABSTRACT

Introduction: HIV-1 infection is considered one of the major public health problems worldwide. Due to the limited access to antiretroviral therapy, the associated side effects, and the resistance that the virus can generate, it has become necessary to continue the development of new antiviral agents. Natural products and their derivatives have shown therapeutic potential against HIV-1, including zidovudine, bevirimat, calanolide A, among others. The present study aimed to identify the anti-HIV-1 potential (*in vitro* and *in silico*) of sixteen synthetic di-halogenated compounds derived from L-Tyrosine.

Methodology: toxicological modeling was performed with ADMET Predictor® and molecular docking with viral proteins was evaluated *in silico* using Autodock Vina®. *In vitro* cytotoxicity was determined by MTT in the TZM-bl cell line. A combined antiviral screening strategy (pre- and post-infection treatment) was performed in HIV-1 infected TZM-bl cells (R5 and X4 strains). The inhibitory effect was quantified by luciferase activity. Moreover, the antiviral activity of the most promising compounds against a pseudotyped virus (HIV-GFP-VSV-G) was determined by flow cytometry.

Results: lower toxicity (both *in silico* and *in vitro*) of L-tyrosine-derived compounds was observed for those compounds with the free OH compared to tyramine-derived compounds. The compounds TODB-2M, TODC-2M, TODC-3M and YDC-3M showed statistically significant inhibitory activity greater than 40% against HIV-1 strains X4 and R5, and greater than 12% against HIV-GFP-VSV-G virus. Finally, *in silico* results showed favorable binding energy, mainly with protease, reverse transcriptase or gp120.

Conclusion: compounds TODB-2M, TODC-2M, TODC-3M and YDC-3M have antiviral potential against HIV-1. The antiviral activity may be due to interaction with reverse transcriptase and/or viral protease, or with envelope gp120.

Keywords: HIV-1, antiviral, cytotoxicity, molecular docking, L-tyrosine derivatives.

ABBREVIATIONS

μl	Microliter
μM	Micromolar
ABC	Abacavir
ADT	Autodock tools
AIDS	Acquired immunodeficiency syndrome
ALP	Alkaline phosphatase
ANOVA	Analysis of variance
ART	Antiretroviral therapy
AZT	Zidovudine
CA	Capsid
cART	Combination antiretroviral therapy
CC50	50% cytotoxic concentration
CFR	Circulating recombinant forms
DMEM	Dulbecco's Modified Eagle's Medium
DMSO	Dimethyl sulfoxide
DTG	Dolutegravir
EDTA	Ethylenediaminetetraacetic acid
EFV	Efavirenz
FBS	Fetal bovine serum
FDA	Food and Drug Administration
FTR	Fostemsavir
GGT	Gamma-glutamyltransferase

HIV	Human immunodeficiency virus
IN	Integrase
INSTIs	Integrase strand transferase inhibitors
LDH	Lactate dehydrogenase
LPV	Lopinavir
LTR	Long terminal repeat
MA	Matrix
mg	Milligram
mL	Milliliter
MTT	(3-(4,5- Dimethylthiazol-2-yl)-2,5-diphenyltetrazolium bromide)
MVC	Maraviroc
NC	Nucleocapsid
ng	Nanogram
NNRTI	Non-nucleoside reverse transcriptase inhibitor
NRTIs	Nucleoside/Nucleotide reverse transcriptase inhibitors
PBMC	Peripheral blood mononuclear cells
PBS	Phosphate-Buffered Saline
PDB	Protein data bank
PI	Protease inhibitor
PMV	Python Molecular Viewer
PR	Protease
RAL	Raltegravir
RLU	Relative light units

RT	Reverse transcriptase
RTV	Ritonavir
SGOT	Aspartate Aminotransferase
SGPT	Alanine Aminotransferase
SI	Selectivity index
ssRNA	Single-stranded ribonucleic acid
T20	Enfuvirtide
UNAIDS	United Nations Program on HIV/AIDS

INTRODUCTION

Human immunodeficiency virus (HIV) is responsible for one of the most devastating human pandemics. From the beginning of the epidemic in 1981 [1], to the present day, HIV has infected around 79 million people worldwide [2].

According to the United Nations Program on HIV/AIDS (UNAIDS) report, in 2021, 38.4 million people were living with HIV, and 1.5 million contracted the infection last year. An estimated 28.7 million people (74.7% of those infected) had access to antiretroviral therapy. Despite global efforts to reduce HIV/AIDS-related deaths and the implementation of antiretroviral therapy (ART), there were nearly 680,000 deaths from acquired immunodeficiency syndrome (AIDS)-related illnesses by 2020 [2].

In Colombia, the high-cost account estimates 134,636 people living with HIV. In 2021, 13,864 new cases were reported and antiretroviral treatment coverage was 95.28% [3].

Combination antiretroviral therapy (cART) successfully suppresses HIV viral load, increases the number of CD4⁺ T lymphocytes, restores immune function, prevents HIV transmission, avoids resistance, prevents clinical progression of the disease, and improves the quality of life [4]. Given these advances, UNAIDS has set a target of "95-95-95" by 2030, to have 95% of HIV-infected people know their HIV status, 95% of those diagnosed have access to treatment, and 95% of those on ART achieve undetectable viral load [5]. cART acts on different steps of the HIV replication cycle. This therapy includes two nucleoside reverse transcriptase inhibitors (NRTIs) combined with an integrase inhibitor, a protease inhibitor (PI), or a non-nucleoside reverse transcriptase inhibitor (NNRTI) [6, 7].

Due to adherence problems and toxic effects, prolonged treatment with combination therapies can be challenging to sustain. Strict adherence is necessary to achieve virological success; lack of adherence can increase viral resistance to antiretroviral drugs and transmission of drug-resistant strains of HIV [8]. However, drug resistance can also appear during treatment. This acquired resistance is observed in patients with a more extended time of treatment; but this resistance also depends on the genetic barrier for each drug, which is defined by the number of mutations required to cause resistance [9, 10]. Adherence often depends on the complexity of therapeutic regimens, side effects, personal habits, depression,

other comorbidities, or conditions specific to each patient [11]. All antiretroviral drugs can have both short-term and long-term adverse effects. Adverse effects are related to each compound, host genetic factors and patient lifestyle [12]. These include an increased risk of cardiovascular, renal, hepatic, and neurological diseases [12-14].

Thus, the continued development of new drugs with high potency against new therapeutic targets, with improved efficacy and safety profile, is a priority. The development of new therapies will help increase the number of new drugs available and broaden the scope of combination therapy.

General aspects of the HIV-1 infection

HIV-1 is a lentivirus, a member of the *Retroviridae* family which are positive-sense single-stranded ribonucleic acid (ssRNA) viruses. The genome is about 9.3 kb in size [15].

Two distinct species of HIV have been identified: HIV-1 and HIV-2. HIV-1 has been further disrupted into four virus groups: M, N, O, and P. Group M is the predominant circulating HIV-1 and is responsible for the pandemic, this group is further subdivided into nine subtypes (A-K), and the missing subtypes E and I belong to circulating recombinant forms (CFR) [16, 17].

HIV-1 is transmitted via direct viral exposure at mucosal surfaces and percutaneous inoculation. The virus is found in blood, semen, pre-seminal fluid, rectal and vaginal fluids, and breast milk [18, 19].

HIV infects all CD4⁺ cells, including T lymphocytes, dendritic cells, monocytes, and macrophages. Once infected, CD4⁺ cells have a shorter half-life and are destroyed by various mechanisms. With the increasing depletion of this population, due to depletion of lymphoid precursors, fibrosis of lymphoid tissues and chronic immune activation, as well as dysregulation of B-cell function, the immune system fails, and the individual becomes susceptible to opportunistic infections and cancer [20, 21].

HIV-1 replication steps

Virus entry into the host cell initiates with the binding of gp120 to the CD4 cell receptor and the interaction with the co-receptor (CCR5 or CXCR4); then gp41 mediates the fusion of cell membrane and viral envelope. HIV can be classified based on its co-receptor binding: CCR5 binding (R5-tropic HIV), CXCR4 binding (X4-tropic HIV), and both R5X4 (dual-tropic HIV) [22].

After entry, the p24 protein is disorganized and the contents of the viral particle are released into the cytoplasm. The single-stranded RNA is then converted to double-stranded DNA by the action of the viral reverse transcriptase (RT) enzyme [23]. The newly synthesized DNA strand is then imported into the host cell nucleus by the viral protein R (Vpr) action. In addition to being involved in nuclear transport, this viral protein is responsible for G2 cell cycle blockade of dividing cells and transcriptional modulation of immune function [24]. Once in the nucleus, the viral enzyme integrase (IN) is responsible for transferring the viral DNA into the host cell genome. After insertion, the HIV provirus can either remain dormant or be actively transcribed [23, 25].

Once the viral DNA is integrated, it is transcribed into an incompletely spliced mRNA. The viral regulatory proteins Tat and Rev, which are essential for replication, act at this point. Tat protein binds to RNA sequences and activates transcription, increasing HIV gene expression. Rev protein facilitates the nuclear export of spliced and unspliced viral mRNA [23]. Then, in the cytoplasm it is translated into the different Gag and Gag-Pol polyproteins. The viral RNA and proteins come to the cell surface and assemble into an immature virion. Finally, plasma membrane budding and viral maturation occur, where polyproteins are cleaved into the different proteins: Matrix (MA), capsid (CA), nucleocapsid (NC), p6, protease (PR), reverse transcriptase (RT), and integrase (IN). Once the virions are budded, they are released into the extracellular space [25, 26].

HIV therapy targets and agents

The Food and Drug Administration (FDA) has played a major role in the progress against HIV/AIDS by streamlining the approval process for antiretroviral drugs, diagnostics, and AIDS vaccines [27].

HIV infection has changed from a fatal disease to a manageable chronic disease with a life expectancy, in some cases, estimated to be close to that of the general population [28].

Currently, the FDA has approved 5 classes of drugs that target different stages of the replication cycle. 1) Entry Inhibitors, 2) NRTIs, 3) NNRTIs, 4) Integration Inhibitors - Integrase strand transferase inhibitors (INSTIs) and 5) Protease Inhibitors (PIs).

Viral entry Inhibitors

They are a group of agents that block viral entry into CD4+ cells through various mechanisms. This group includes attachment inhibitors, CCR5 antagonists, and fusion inhibitors [29].

Attachment Inhibitors

Glycoprotein 120 (gp120) is the protein that is responsible for the HIV entry process in the host cells. It consists of five variable protein domains (V1-V5) interspersed with five relatively constant domains (C1-C5). The viral gp120 protein is composed of an inner and an outer domain connected by a bridging sheet. The conserved domains contribute to the core of gp120, whereas the variable domains are located near the surface of the molecule [30, 31].

Currently, the only FDA-approved drug in this class is Fostemsavir. Temsavir, the active metabolite of fostemsavir, binds directly to gp120 near the CD4 binding site and blocks gp120 in a closed state that prevents the conformational change necessary for the initial interaction between the virus and surface receptors on CD4 cells [32, 33]. It is widely used for patients with multidrug-resistant HIV-1 infection [34]. Fostemsavir is well tolerated; the most frequent adverse effects include headache, nausea, and diarrhea [33, 35].

Co-receptor antagonists

The chemokine receptors CXCR4 and CCR5 function together with CD4 to facilitate viral entry into target cells. Maraviroc (MVC) acts as an antagonist of the HIV-1 co-receptor CCR5 by blocking its interaction and binding with gp120 and the membrane fusion events required for HIV-1 tropism-CCR5 entry into human cells [36, 37]. It is a drug usually very well tolerated, with an excellent metabolic and digestive tolerability profile; adverse effects include headache, dizziness, rhinitis, and nausea [38].

Fusion Inhibitors

Glycoprotein 41 (gp41) mediates the fusion of the viral envelope with the target cell membrane. It is organized into three main domains: an extracellular domain, a transmembrane domain, and a C-terminal cytoplasmic tail. The extracellular domain contains an N-terminal hydrophobic region known as the fusion peptide, a polar region, and heptad repeat regions HR1 and HR2, which are fusion determinants [30, 39].

FDA-approved enfuvirtide (T20) is the only drug in this class approved by the FDA for the treatment of HIV. T20 is an HR2 mimetic peptide that competes by binding to HR1, blocking the conformational changes required for membrane fusion [40, 41]. As it is a drug administered subcutaneously, the most common adverse effect is the appearance of painful macules, itching, and induration of the injection site [42].

Reverse transcriptase inhibitors

Reverse transcriptase (RT) is an RNA-dependent DNA polymerase that produces double-stranded DNA from single-stranded RNA. RT is a heterodimeric enzyme comprising a regulatory subunit (p51) and a catalytic subunit (RNase H - p15) that form the p66 molecule [43], consisting of the finger, palm, and thumb subdomains. Additional domains include the connexin and the C-terminal RNase H domain [43, 44].

This group includes nucleoside-nucleotide RT inhibitors (NRTIs) and non-nucleoside RT inhibitors (NNRTIs).

Nucleoside/Nucleotide RT Inhibitors (NRTIs)

Inhibits reverse transcription of viral RNA to double-stranded DNA. Prevents elongation during reverse transcription using deoxyribonucleosides lacking a 3'-OH. Upon DNA transcription, it terminates strand growth and stops DNA synthesis by competing with the natural substrate dNTP [45, 46].

Currently, the available FDA-approved NRTIs are zidovudine, didanosine, zalcitabine, stavudine, lamivudine and abacavir, Tenofovir disoproxil fumarate, Emtricitabine, Tenofovir alafenamide fumarate [47, 48].

The most frequent adverse reactions in this group of drugs are hypersensitivity reaction, mitochondrial toxicity, myopathy, lactic acidosis, pancreatitis, peripheral neuropathy, anemia, hepatic steatosis, and lipodystrophy [6, 12].

Nonnucleoside RT Inhibitors (NNRTIs)

It blocks the completion of reverse transcription by binding to the binding pocket near the catalytic residues of the reverse transcriptase active site, thereby inducing a conformational change that inactivates the enzyme [45].

The NNRTIs approved for the treatment of HIV-1 are delavirdine, doravirine, efavirenz, etravirine, nevirapine, and rilpivirine [47]. Hypersensitivity reactions, skin rash, headache, and depression have been found in this class of inhibitors [6, 12, 48].

Integrase strand transferase inhibitors (INSTIs)

Integrase is a protein composed of three structural and functional domains. An N-terminal zinc-binding, a catalytic center (which contains the active site residues Asp64, Asp116, and Glu152), and a C-terminal DNA-binding. This enzyme cleaves the 3'-OH group and then transfers the viral strand to the host chromosome for integration [49].

Integrase inhibitors bind to the catalytic domain and block the strand transfer reaction, preventing the viral genome from inserting into the DNA of a host cell [50].

The FDA-approved INSTIs are: Raltegravir, elvitegravir, dolutegravir, bictegravir, cabotegravir. This group of drugs has been characterized as having a higher potency than the others and are generally well tolerated. Neurological, weight gain, and gastrointestinal effects have been described [51].

Inhibitors of the Viral Maturation - Protease inhibitors (PIs)

HIV protease (PR) is an aspartic protease active as a homodimer. The active site is between the two subunits and has the triad, Asp25-Thr26-Gly27. The two D25 residues (one on each chain) act as catalytic residues [52]. This enzyme cuts the Gag and Gag-Pol precursor proteins for virion maturation. PIs bind to HIV-1 protease and block proteolytic cleavage of protein precursors required to produce infective viral particles [53].

Currently approved for use are saquinavir, ritonavir, indinavir, nelfinavir, amprenavir, lopinavir, atazanavir, fosamprenavir, tipranavir and darunavir. PIs are disadvantaged by the number of adverse effects they can produce, including lipodystrophy, dyslipidemia, transaminitis, and hepatotoxicity [12].

Natural compounds and derivatives with antiviral activity against HIV

Natural products are an important source for the development of pharmaceuticals. In fact, a high percentage of FDA-approved drugs are derived directly or indirectly from natural products [54]. HIV treatment has limitations; therefore, finding new anti-HIV compounds with accepted toxicity and a lower resistance profile is a pressing need.

In this section, natural products with potential anti-HIV activity and putative mechanisms of action were reviewed and compiled. These compounds were mainly isolated or derived from plants and marine sponges. This review focuses on terpenes, coumarins, flavonoids, laccases, lectins, ribosome-inactivating proteins (RIPs) and bromotyrosines.

This specific section containing this information was reviewed in **Review: Natural Products with Inhibitory Activity against Human Immunodeficiency Virus Type 1**. Serna-Arbeláez MS, Florez-Sampedro L, Orozco LP, Ramírez K, Galeano E, Zapata W. *Adv Virol*. 2021 May 29; 2021:55520 DOI: 10.1155/2021/5552088. PMID: 34194504; PMCID: PMC8181102 (**Attachment 1**).

Problem statement

Although for several decades there have been multiple specific antiretroviral treatments to control HIV infection, this therapy produces side effects that can lead to problems of adherence. The most common short-term adverse effects of this medication are headache, asthenia, diarrhea and hypersensitivity reactions; at the same time, in the long-term, they have been associated with cardiac, bone and renal complications [12].

The lack of adherence can affect the total inhibition of viral replication, favoring the emergence of resistant strains [55]. This resistance to cART can be primary or transmitted at the time of infection, in the case of patients who have not been previously exposed to the drug, or secondary or acquired resistance which has been described in patients taking these

drugs [55, 56]. For notwithstanding treatment with effective drugs and even when treatment adherence is maintained, some resistance to anti-HIV cART is expected to emerge. This drug resistance differs depending on the class of antiretroviral drugs, as some have a higher genetic barrier than others [56, 57]. HIV drug resistance can affect the efficacy of cART and the duration of the drugs available to treat HIV infection.

Considering the need to adopt new therapeutic approaches against HIV-1, it is necessary to investigate new compounds, easily accessible and inexpensive, with strong antiviral activity and with the least possible side effects.

Natural products have attracted special interest due to the existing biodiversity worldwide. Natural products and their derivatives represent an excellent option due to their therapeutic potential against HIV-1 infection.

The evaluation of the pharmacological properties of compounds isolated from marine sponges dates back to the 1950s, with the purification of nucleotides, isolated from extracts of the sponge *Tectitethya crypta* [58]. A few years later, Zidovudine, the first anti-HIV drug, was synthesized from this nucleotide [59].

Taking this into account, the Marine Natural Products Group of the University of Antioquia researched the Colombian Caribbean sponge species *Aiolochoia crassa* and *Verongula rigida*, which evidenced a wide range of bromotyrosines-like molecules, which showed pharmacological potential as inhibitors of HIV-1 replication *in vitro* [60].

In this context, the active search for compounds that can be used for the treatment of HIV is a worldwide research priority. Therefore, it was proposed to identify the anti-HIV-1 potential (*in vitro* and *in silico*) of sixteen di-halogenated compounds derived from L-tyrosine.

OBJECTIVES

General objective

- To evaluate the *in vitro* and *in silico* antiviral activity against HIV-1 of di-halogenated compounds derived from L-tyrosine.

Specific objectives

- To determine *in silico* possible interactions between compounds and HIV-1 viral proteins.
- To model and analyze the possible *in silico* toxicity of the compounds against HIV-1.
- To evaluate the *in vitro* cytotoxicity of the compounds in susceptible cells for HIV-1 infection.
- To evaluate the *in vitro* antiviral activity of the compounds against HIV-1.

RESEARCH QUESTION

Is there *in silico* and *in vitro* antiviral activity of di-halogenated compounds derived from L-tyrosine against HIV-1?

HYPOTHESIS

Based on evidence from previous studies performed on other compounds structurally related to L-tyrosine derivatives, we hypothesize that some di-halogenated compounds exhibit *in silico* and *in vitro* activity against HIV-1.

MATERIALS AND METHODS

Di-halogenated compounds derived from L-Tyrosine

Two groups of di-halogenated compounds derived from L-Tyrosine were evaluated: L-Tyrosine derivatives and Tyramine derivatives. L-Tyrosine derivatives included those compounds with the free phenolic OH and the methyl ether derivatives of tyrosine, which have their

carboxyl group methylated. Within these, four compounds were evaluated: two dibrominated in the aromatic ring in the ortho positions concerning the phenolic OH and two dechlorinated in the same positions, corresponding to their respective tertiary amine and quaternary ammonium salts (TDB-2M, TDB-3M, TDC-2M, and TDC-3M and TODB-2M, TODB-3M, TODC-2M, and TODC-3M respectively). The Tyramine derivatives compounds were classified in the same way as L-Tyrosine derivatives thus obtaining eight compounds: YDB-2M, YDB-3M, YDC-2M, YDC-3M, and YODB-2M, YODB-3M, YODC-2M, and YODC-3M. The classification of the compounds can be seen in *Figure 1*.

water solution with 5% dimethyl sulfoxide (DMSO) (Sigma-Aldrich, St Louis, MO, USA) at a concentration of 1 mg/mL for the preparation of a mother stock in concentrations dependent on the molecular weight of each compound (according to its chemical nature) (Table 1). Working dilutions were done in Dulbecco's Modified Eagle's Medium-high glucose (DMEM) (Sigma-Aldrich, St Louis, MO, USA) at a concentration of 300 - 9,37 μ M.

Code	IUPAC name	Molecular mass (g/mol)
TDB-2M	(2 <i>S</i>)-3-(3,5-dibromo-4-hydroxyphenyl)-2-(dimethylamino)propanoic acid	338.98
TDB-3M	(1 <i>S</i>)-1-carboxy-2-(3,5-dibromo-4-hydroxyphenyl)- <i>N,N,N</i> -trimethylethan-1-aminium	382.07
TDC-2M	(2 <i>S</i>)-3-(3,5-dichloro-4-hydroxyphenyl)-2-(dimethylamino)propanoic acid	278.13
TDC-3M	(1 <i>S</i>)-1-carboxy-2-(3,5-dichloro-4-hydroxyphenyl)- <i>N,N,N</i> -trimethylethan-1-aminium	293.16
TODB-2M	(2 <i>S</i>)-3-(3,5-dibromo-4-methoxyphenyl)-2-(dimethylamino)propanoic acid	381.06
TODB-3M	(1 <i>S</i>)-1-carboxy-2-(3,5-dibromo-4-methoxyphenyl)- <i>N,N,N</i> -trimethylethan-1-aminium	396.09
TODC-2M	(2 <i>S</i>)-3-(3,5-dichloro-4-methoxyphenyl)-2-(dimethylamino)propanoic acid	292.16
TODC-3M	(1 <i>S</i>)-1-carboxy-2-(3,5-dichloro-4-methoxyphenyl)- <i>N,N,N</i> -trimethylethan-1-aminium	307.19
YDB-2M	2,6-dibromo-4-[2-(dimethylamino)ethyl]phenol	337.05
YDB-3M	2-(3,5-dibromo-4-hydroxyphenyl)- <i>N,N,N</i> -trimethylethan-1-aminium	352.08

YDC-2M	2,6-dichloro-4-[2-(dimethylamino)ethyl]phenol	248.15
YDC-3M	2-(3,5-dichloro-4-hydroxyphenyl)- <i>N,N,N</i> -trimethylethan-1-aminium	263.18
YODB-2M	2-(3,5-dibromo-4-methoxyphenyl)- <i>N,N</i> -dimethylethan-1-amine	351.07
YODB-3M	2-(3,5-dibromo-4-methoxyphenyl)- <i>N,N,N</i> -trimethylethan-1-aminium	366.11
YODC-2M	2-(3,5-dichloro-4-methoxyphenyl)- <i>N,N</i> -dimethylethan-1-amine	262.17
YODC-3M	2-(3,5-dichloro-4-methoxyphenyl)- <i>N,N,N</i> -trimethylethan-1-aminium	277.21

Table 1. Di-halogenated compounds derived from L-tyrosine evaluated in the study.

The positive control of HIV inhibition was zidovudine (AZT) (Sigma Aldrich, St Louis, USA). The AZT concentration was established at 10 μ M after literature consultation [62], and untreated cells were used as a negative control.

Cell maintenance

TZM-bl cells were obtained from the NIH AIDS Research and Reference Reagent Program (Cat. no. 8129). This cell line is derived from a clone of HeLa cells designed for expressing HIV-1 virus entry co-receptor (CD4 CXCR4 and CCR5) with an integrated luciferase gene under the control of the HIV-1 promoter long terminal repeat (LTR) [63, 64], which makes it possible to measure infection. The cells are highly permissive to infection by most strains of HIV, including primary viral isolates and pseudotyped viruses [65]. TZM-bl cells were cultured at 37°C with 5% CO₂ in DMEM supplemented with heat-inactivated fetal bovine serum (FBS) (Sigma-Aldrich, St. Louis, MO, USA). Cell monolayers were detached by treatment with Trypsin ethylenediaminetetraacetic acid (EDTA) solution of 0.25% (Sigma-Aldrich, St. Louis, MO, USA).

HEK293T is a derivative cell line of the human embryonic kidney that expresses the SV40 large T antigen, which enables them to produce recombinant retroviruses. These cells were

maintained in DMEM (Sigma-Aldrich, St Louis, MO, USA) containing 10% FBS and 2mM glutamine (Sigma-Aldrich, St. Louis, MO, USA). Cells were incubated at 37°C in a humidified environment of 5% CO₂. Cell monolayers were detached by treatment with Trypsin EDTA solution 0.25%. In these cells, transfection assays to produce pseudotyped virus were performed.

H9/HTLV-III_B cells (ATCC-CRL-8543) of lymphoblastoid origin were maintained in RPMI-1640 medium (Sigma-Aldrich, St. Louis, MO, USA), supplemented with 10% FBS, and were incubated in a humid atmosphere with 5% CO₂ at 37°C. This cell line is persistently infected and was used to produce HIV-1_{III_B} (X4-tropic HIV-1) viral stocks.

Human peripheral blood mononuclear cells (PBMC) from two healthy donors were obtained from the blood bank of the Hospital Universitario San Vicente Fundación. PBMC were isolated through density gradient with Ficoll-Histopaque (Sigma-Aldrich, St. Louis, MO, USA) by centrifugation at 400g for 30 minutes; then PBMCs were washed 3 times with Phosphate-Buffered Saline (PBS) (Lonza, Rockland, ME, USA) to eliminate platelets and debris. After, cells were counted and frozen until they were used. PBMCs were thawed and let in culture for 24 h before each experiment.

Production of viral stocks

R5-tropic HIV-1 was obtained through the NIH HIV Reagent Program, Division of AIDS, NIAID, NIH: Human Immunodeficiency Virus Type 1 (HIV-1) BaL, ARP-510, contributed by Dr. Suzanne Gartner, Dr. Mikulas Popovic and Dr. Robert Gallola [66]. Viral stocks were obtained after propagation in the presence of 10 µg/ml polybrene (Sigma Aldrich, St Louis, USA) in PBMCs stimulated with 5 µg/ml of Phytohemagglutinin- PHA (Sigma-Aldrich, St. Louis, USA) and 20 U/ml IL-2 (R&D Systems, MN, USA) and cultured with RPMI medium supplemented with 10% FBS.

X4-tropic HIV-1_{III_B} was obtained from the HIV-1 chronically infected human T cell line III_B (H9/HTLV-III_B) (ATCC-CRL-8543). Supernatants were collected and stored at -70°C for viral titration.

Pseudotyped HIV-1 virus stocks were produced in HEK293T cells by co-transfection of pNL4-3 delta env GFP (HIVΔenv.GFP) and pVSV-G plasmids encoding for full-length HIV-

1 NL4-3 proviral DNA with a frameshift in the env gene and expressing GFP instead of nef and for vesicular stomatitis virus G protein, respectively. These plasmids were kindly provided by Johnny He [67, 68]. For this procedure, HEK293T cells (4.5×10^5 cells/well) were seeded in 6-well plates, 24 h later co-transfected with 3.2 μg of HIV Δ env.GFP and 0.8 μg of pVSV-G per well-using lipofectamine 3000 (Invitrogen, USA) for 4 h in the presence of Opti-MEM medium (Gibco, Grand Island, NY), after which time the DNA-lipofectamine complex was removed and 2ml/well DMEM supplemented 10% with FBS was added. The supernatants containing virus stocks HIV-GFP-VSV-G reporter virus, were collected 72 h after transfection and centrifuged at 500 g for 10 min to remove cell debris. A Lenti X concentrator (Clontech, Mountain View, CA, USA) was used to concentrate the supernatants, and these were stored at -70°C for subsequent titration and use. Cells were directly observed under an Olympus 10-fold objective lens microscope (Zeiss). Fluorescence images were observed using the GFP filter cube.

Quantification of p24 by ELISA.

The supernatants obtained in the production of the different viral stocks were collected for titration by p24 estimation using an ELISA kit (XpressBio, Ballenger Creek, Maryland, USA), following the manufacturer's instructions.

Determination of cytotoxicity

The *in vitro* cytotoxic effect of the di-halogenated compounds on TZM-bl cells was determined by the MTT (3-(4,5- Dimethylthiazol-2-yl)-2,5-diphenyltetrazolium bromide) assay (Sigma-Aldrich, St. Louis, MO, USA). For this purpose, 1.2×10^5 cells/well were seeded in 96-well plates, which were incubated at 37°C and 5% CO_2 for 24 h. DMEM was used as a negative control and serial two-fold dilutions of the compounds were performed at 9.37 to 300 μM in DMEM supplemented with 5% FBS. 100 μL /well of each dilution was added and incubated for 48 h. Subsequently, the cells were washed 2 times with 1X PBS, and 30 μl of MTT solution (2 mg/mL) was added and incubated for 2 h at 37°C , in a light-protected culture. Then, 100 μl of DMSO was added to dissolve the formazan crystals, placed in shaking for 15 min and absorbance reading was performed at 570 nm, using the Microplate Spectrophotometer (Thermo Scientific™ Multiskan™ GO). Each experimental condition

was evaluated in quadruplicate in two independent experiments (n=8). The percentage of viability was calculated concerning the absorbance of the controls without compound (100% viability). The 50% cytotoxic concentration (CC₅₀) was calculated and analyzed with GraphPad Prism version 8.0.1 (GraphPad Software, Inc.).

Antiviral screening

As a strategy for the determination of the antiviral effect of compounds, an antiviral screen was performed in TZM-bl cells. For this, cells were seeded in a flat-bottom 96-well plate (Corning, NY, USA) at the concentration of $1,2 \times 10^5$ cells/well and incubated for 24 h at 37°C before the addition of each compound at non-cytotoxic concentrations (pre-infection treatment). 1 hour later the treatment was removed, and infection was performed by adding 10 ng/ml of HIV-1_{IIIB} p24 (X4) or 2 ng/ml of HIV-1 BaL (R5) to the monolayers which were incubated for 3hrs; finally, the viral inoculum was removed, washed with 1x PBS and the compounds were added again (post-infection treatment). Additionally, three wells were left for the negative control (cells without treatment or infection), the positive control of infection (cells infected with the virus without treatment), and the positive control of inhibition (AZT). Antiviral activity was quantified 48 hours after treatment by measuring luciferase activity, which is directly proportional to the number of infectious virus particles in the sample [69].

The luciferase activity was quantified by luminescence emitted by the cells using Bright-GloTM Luciferase Assay System (Promega Corp., Madison, WI) following the manufacturer's instructions. Briefly, 100 ul of the reagent is added to 100 ul of TZM-bl cells and incubated for at least 2 min protected from light. Relative light units (RLUs) were measured using the multi-mode plate reader (Thermo ScientificTM VarioskanTM LUX). Each experimental condition was performed in triplicate in two independent experiments (n=6).

The percentage inhibition was calculated as follows: $100 - (\text{RLU of treated cells} - \text{RLU of uninfected cells} / \text{RLU of infection control} - \text{RLU of uninfected cells}) * 100$.

VSV-pseudotyped HIV-1 infection assay and quantification of the percentage of infected cells by flow cytometry

TZM-bl cells were seeded in a 96-well plate at the concentration of $1,2 \times 10^5$ cells/well 1 day before infection, then inoculated with HIV-GFP-VSV-G reporter virus stocks (40 ng of p24) in the presence of 10 μ g/ml polybrene (Sigma Aldrich, St Louis, USA) for 3 hours. Cells were washed twice with 1X PBS and treated with the most bioactive compounds at non-cytotoxic concentrations for 48 hours; finally, cells were trypsinized and rewashed with PBS. Antiviral activity was quantified by flow cytometry for GFP.

TZM-bl VSV-pseudotyped HIV-1-infected cells and TZM-bl control cells, as described above, were used to measure the percentage of infection by flow cytometry for GFP expression. Cells were acquired using LS Fortessa (BD Biosciences, San Jose, CA, USA) and data were analyzed using FlowJo version 10.5.3 (FlowJo, LLC, Oregon, USA).

The percentage of inhibition was calculated as follows: $100 - (\text{Infection percentage in treated cells} \times 100 / \text{percentage in control infection})$.

Evaluation of the interaction of compounds with viral proteins by molecular docking

Ligand preparation

The structure of the di-halogenated compounds derived from L-tyrosine was obtained with the program ACD/ChemSketch® 12.01 (Freeware Version), and the structure of the control compounds from the DrugBank database (<https://www.drugbank.ca/>). The geometry of all compounds was optimized using Avogadro software in the lowest energy conformation using the MMFF94 force field [70, 71].

The ligands were prepared for docking was performed using Autodock tools (ADT) program [72], where the charges and degrees of torsion were added.

Protein preparation

For molecular docking, three-dimensional structures of structural and non-structural viral proteins were downloaded from the PDB (Protein Data Bank), and structures with a resolution equal to or less than 2.5 Å were considered.

The seven HIV-1 viral proteins chosen for analysis were: gp120 (PDB: 4J6R), gp41 (PDB: 3VTQ), RT (PDB: 4G1Q), IN (PDB: 1QS4-3OYA), protease (PDB: 5YOK), p17 (PDB: 4JMU) and p24 (PDB: 2XDE). For the integrase structure, the 1QS4 structure, which has one of the Mg²⁺ of the active site, was initially taken as a basis. The missing residues were incorporated [73] and the second magnesium ion was placed in the same relative position according to the two metal structures of the Prototype Foamy Virus integrase (PDB code 3OYA) [74].

The 3D models of interest were prepared for docking using the Python Molecular Viewer (PMV) software [75], removing both water molecules and co-crystallized molecules that were not part of the target protein, adding Gasteiger charges, adding non-polar hydrogens, and the torsional degrees of freedom were also assigned by the ADT program [72].

To determine the possible molecule binding sites on these proteins, the PeptiMap server [76, 77] was used and based on these sites, box coordinates with 1 Å spacing and number of points at xyz = 30 were defined and evaluated with the completeness of 10.

Finally, to determine the best interactions between the viral proteins and the compounds, Autodock Vina software [78] was used.

Several authors have considered -6.0 Kcal/mol as a cut-off point in ligand binding studies [79-81]. Considering this, our study established a score lower than the upper threshold ($\Delta G_{bind} = -6.0$ Kcal/mol), determining that a ligand-protein interaction is strong. Evaluation of possible interactions was performed by PMV and Discovery Studio software [82]. *Table 2* shows the viral proteins evaluated in the study and the amino acids that were used as targets for molecular docking.

Protein	PDB code	Resolution (Å)	Sequence length	Chain	Active site amino acids
gp120	4J6R	1.64	359	G	W112, T257, D368, E370, S375, F382, I424, M426, W427, M434, M475
gp41	3VTQ	1.53	37	N	L565, L566, T569, V570, W571, G572,

					I573, K574, L576, Q577.
RT	4G1Q	1.51	557	A	D110, Y183, D185, D186, L100, K101, K103, V106, T107, V108, V179, Y181, Y188, V189, G190, F227, Y318, E138.
Protease	5YOK	0.85	100	A-B	D25, T26, G27
Integrase	1QS4	2.1	154	A	D64, D116, E152
p24	2XDE	1.4	145	A	F32, E35, V36, N57, V59, E60, H62, Q63, A65, Q67, K70, T107, M118, T119
p17	4JMU	2.0	112	A	L21, R22, P23, Y29, K32, H33, W36, S77, L88, N80, T81, T81, T97, K98, L101

Table 2. Viral proteins and binding sites are defined in the study as targets for molecular docking with the compounds.

***In silico* toxicological modeling**

In silico toxicological modeling of halogenated molecules derived from L-Tyrosine was performed using ADMET Predictor® v8 software from Simulation Plus [83], which predicts toxicity parameters in different biological models.

For this, the structures of the molecules were modeled in the ACD/ChemSketch ®12.01 (Freeware Version) program, the geometry optimized using the Avogadro software and subsequently, they were entered into the ADMET Predictor® software, which issued the results of the parameters of interest defined in the study.

For the toxicological evaluation, in addition to the compounds and control drugs evaluated, we used a compound that was called "ideal", which is hypothetical, to compare the toxicity

among all the compounds. With these results, a hierarchical cluster analysis (Ward's method, Bray-Curtis similarity index) was performed with R [84].

Moreover, the score of the potential toxicity level of each compound was defined on a scale from 0 to 13 and was reported as cumulative toxicity, according to the sum of the qualitative result of each parameter, whether it was toxic (T) one (1) point, or non-toxic (N) zero (0) points and was classified as low: 1 to 4 positive toxic parameters, medium: 5 to 8 positive toxic parameters, and high: 9 to 13 positive toxic parameters.

Statistical analysis

The CC_{50} will be defined as the concentration of each compound that can reduce cell viability to 50% of the untreated cell control. The IC_{50} will be defined as the compound concentration that can reduce viral infection to 50% of the control infected cells not treated with the compounds. The therapeutic selectivity index (SI) will be determined as the ratio of the CC_{50} to the IC_{50} .

The results of the experiments will be expressed as means \pm SD of at least 2 independently performed experiments. Differences between groups were analyzed using one-way analysis of variance (ANOVA) since the data were normally distributed and statistically significant differences with a p-value less than 0.05 were considered for all cases. Data were analyzed on the GraphPad Prism v.8.0.1 software (San Diego, CA, USA).

RESULTS

Di-halogenated compounds derived from L-tyrosine have no significant cytotoxic effect on TZM-bl cells.

Cytotoxicity of the compounds was determined by the MTT assay, using the cell line TZM-bl. In the treatments with the TDB-2M, TODB-2M, TODC-2M, and TODC-3M compounds, lower cytotoxicity was observed as the concentrations decreased, in a dose-dependent manner (*Figure 2A-B*). All tyrosine-derived compounds exhibited cytotoxicity $\leq 10\%$ (with viability greater than or equal to 90%) at a concentration of 150 μM , except for TODB-3M whose cytotoxicity at this concentration was less than 20%. L-Tyrosine-derived compound

that presented the highest viability was TDC-2M at 75 μ M (115%), while the lowest viability was of compound TODB-2M at a concentration of 300 μ M (67.7%).

Figure 2C-D shows that as the concentration of tyramine-derived compounds increased, there was a dose-dependent increase in cytotoxicity, except for YDC-2M, YDC-3M, and YODC-3M compounds. All compounds in this group exhibited cytotoxicity $\leq 30\%$ (with viability greater than or equal to 77%) at a concentration of 150 μ M, except for YDB-3M, whose cytotoxicity was higher. The maximum and minimum viability for this compound was 91.6% and 21.4% at concentrations of 37.5 μ M and 300 μ M, respectively. Therefore, the optimal concentration to be evaluated for YDB-3M was determined to be less than or equal to 75 μ M. Maximum viability was 133% and was observed for YDB-2M at a concentration of 9.375 μ M. Neither the viral inhibition control (AZT) nor the solvent (DMSO) were toxic (*Supplementary figure 1*).

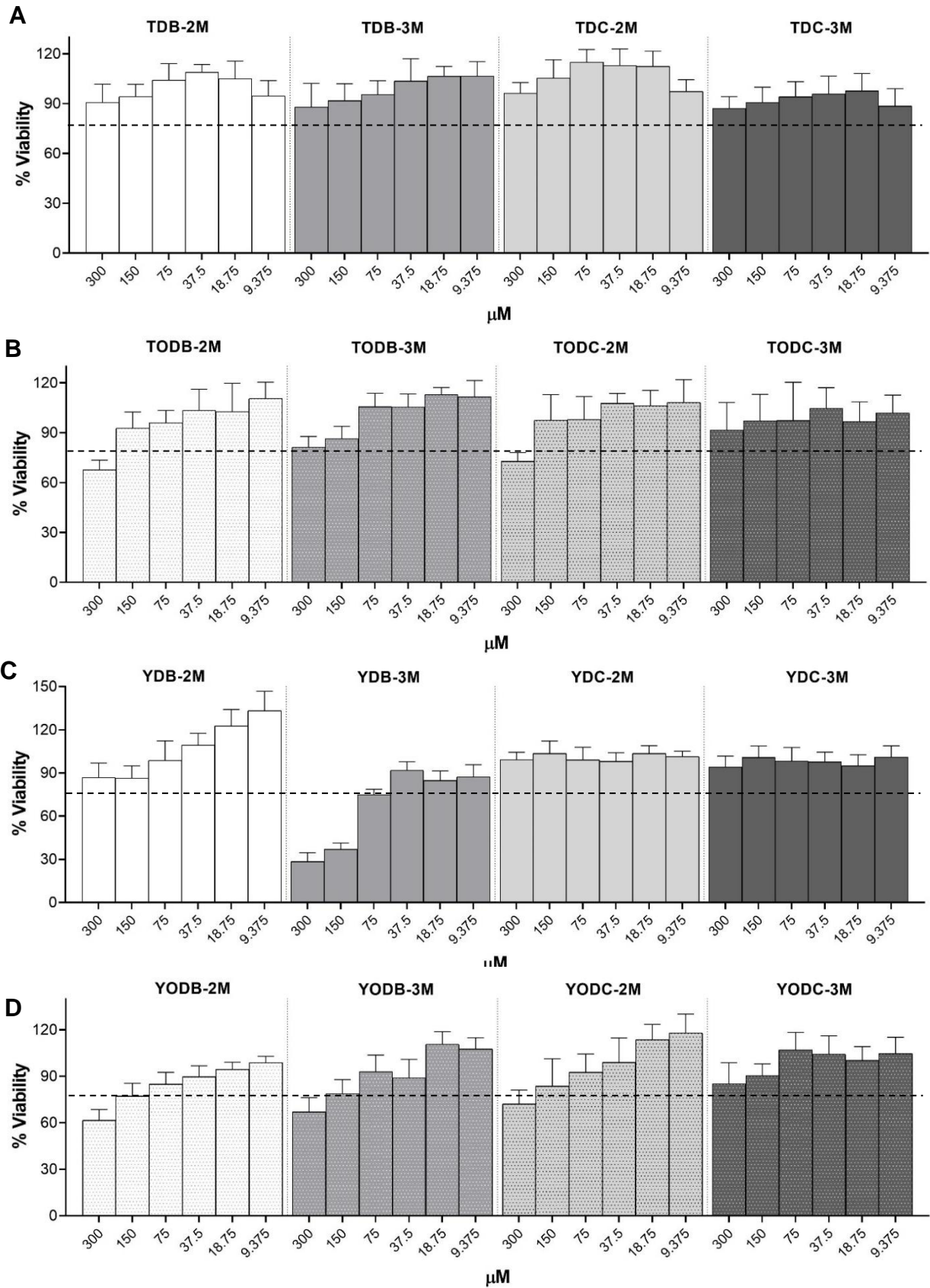


Figure 2. TZM-bl cells treated with tyrosine-derived di-halogenated compounds. A. L-tyrosine with free phenolic OH derivatives. **B.** L-tyrosine methyl ether derivatives. **C.** Tyramine with free phenolic OH derivatives. **D.** Tyramine methyl ether derivatives. TZM-bl cells were treated with different concentrations of each compound (9.37 μM up to 300 μM for 48 h). Percentage viability was calculated relative to untreated cells. Each sample was tested in triplicate in two independent experiments; the results have shown as mean \pm standard deviation. The dotted line indicates 80% of viability.

Considering the low cytotoxicity of the compounds tested and the availability, subsequent assays were performed at non-cytotoxic concentrations. The CC_{50} values for each treatment are shown in *Table 3*.

Group	Compound	CC_{50} (μM)
L-tyrosine derivates	TDB-2M	~ 98,99
	TDB-3M	74,76
	TDC-2M	~ 174,4
	TDC-3M	>300
	TODB-2M	164,9
	TODB-3M	~ 103,6
	TODC-2M	>300
	TODC-3M	74,9
Tyramine derivates	YDB-2M	37,52
	YDB-3M	~ 100,9
	YDC-2M	~ 101,0
	YDC-3M	39,88
	YODB-2M	139,8
	YODB-3M	78,7
	YODC-2M	74,94
	YODC-3M	132,4

Table 3. Cytotoxic concentration of the compounds evaluated.

Di-halogenated compounds showed low *in silico* toxicity.

In silico toxicity modeling for all compounds and control drugs was performed by ADMET Predictor®, and the findings are described in *Table 4*. The results showed that the quaternary ammonium salts TDB-3M and TDC-3M that present within their structure 3 methylations in the amino group, and the compounds YDB-2M, YDB-3M, YDC-2M, and YDC-3M, as well

as YODC-2M, have genotoxic potential (indicated by chromosomal aberration score) as well as the drug zidovudine.

	TDB-2M	TDB-3M	TDC-2M	TDC-3M	TODB-2M	TODB-3M	TODC-2M	TODC-3M	YDB-2M	YDB-3M	YDC-2M	YDC-3M	YODB-2M	YODB-3M	YODC-2M	YODC-3M	ABC	DTG	EFV	FTR	LPV	RAL	RTV	AZT	
Chromosomal aberrations	0	1	0	1	0	1	0	1	1	1	1	1	0	0	1	0	1	0	0	0	0	0	0	0	1
Skin sensitization	1	1	0	0	1	1	0	0	1	1	1	0	1	1	0	0	1	1	1	0	0	1	0	1	1
Respiratory sensitization	0	0	0	0	1	0	1	0	1	1	1	1	1	1	1	1	1	0	1	0	0	0	0	0	0
Neurotoxicity	0	0	0	0	0	0	0	0	0	0	0	0	1	1	1	1	0	0	1	0	0	0	0	0	0
Cardiac toxicity	0	0	0	0	0	0	0	0	0	0	0	0	1	1	1	1	0	0	0	0	0	0	0	0	0
Endocrine tox (estrogen receptor)	1	1	1	1	1	1	1	1	1	1	1	1	0	0	0	0	0	0	0	1	0	0	0	0	0
Endocrine tox (androgen receptor)	0	0	0	0	1	1	1	1	1	1	1	1	0	1	0	1	0	0	1	0	1	0	1	0	0
ALP increase	0	0	0	0	0	0	0	0	0	0	0	1	0	0	0	0	1	0	1	0	1	0	1	1	1
GGT increase	1	0	0	0	1	0	0	0	1	0	0	0	1	0	0	0	0	0	0	0	1	0	1	1	1
LDH increase	0	0	0	0	0	0	0	0	0	0	1	1	1	1	0	0	0	0	0	0	1	0	1	1	1
SGOT increase	0	0	0	0	0	0	0	0	0	0	0	0	0	0	0	0	1	1	1	0	0	1	0	1	1
SGPT increase	0	0	0	0	0	0	0	0	0	0	0	0	0	0	0	0	1	0	1	0	1	0	1	1	1
Reproductive tox	0	0	0	0	0	0	0	0	1	0	0	0	0	0	0	0	0	0	1	0	1	0	1	1	1
Accumulated tox	3	3	1	2	5	4	3	3	7	5	6	6	6	6	4	4	6	2	8	1	6	2	6	8	
ADMET_Risk	0,0	0,9	0,0	1,0	0,0	0,7	0,9	1,4	0,0	0,3	2,0	2,8	0,5	0,4	2,3	1,8	1,4	0,0	4,7	5,0	7,5	2,5	9,7	5,4	

Table 4. *In silico* toxicity score of ADMET properties. **ALP:** Alkaline Phosphatase, **GGT:** gamma-glutamyl transferase, **LDH:** Lactate dehydrogenase, **SGOT:** Aspartate Aminotransferase, **SGPT:** Alanine Aminotransferase, **ABC:** Abacavir, **DTG:** Dolutegravir, **EFV:** Efavirenz, **FTR:** Fostemsavir, **LPV:** Lopinavir, **RAL:** Raltegravir, **RTV:** Ritonavir, **AZT:** Zidovudine.

Regarding allergenic toxicity, all brominated compounds were predicted to be skin sensitizers, as were YDC-2M, and the control drugs dolutegravir, efavirenz, raltegravir, and zidovudine. Respiratory sensitizers were the methyl ether L-tyrosine derivatives (TODB-2M and TODC-2M) and all tyramine derivatives compounds, and typically the control drug Efavirenz.

ADMET data indicated that 12 compounds (except methyl ether tyramine-derivatives) could exhibit endocrine toxicity by interacting with estrogen receptors. In contrast, methyl ether L-tyrosine-derivates, tyramine with free phenolic OH derivatives, YODB-2M and YODC-3M compounds could interact with the androgen receptor.

No compound was predicted to cause reproductive toxicity, except YDB-2M and the control drugs efavirenz, lopinavir, ritonavir, and AZT. All methyl ether tyramine-derivatives compounds were predicted to induce a neurotoxic and cardiac effect (indicated by inducing phospholipidosis and having affinity on potassium channels, respectively).

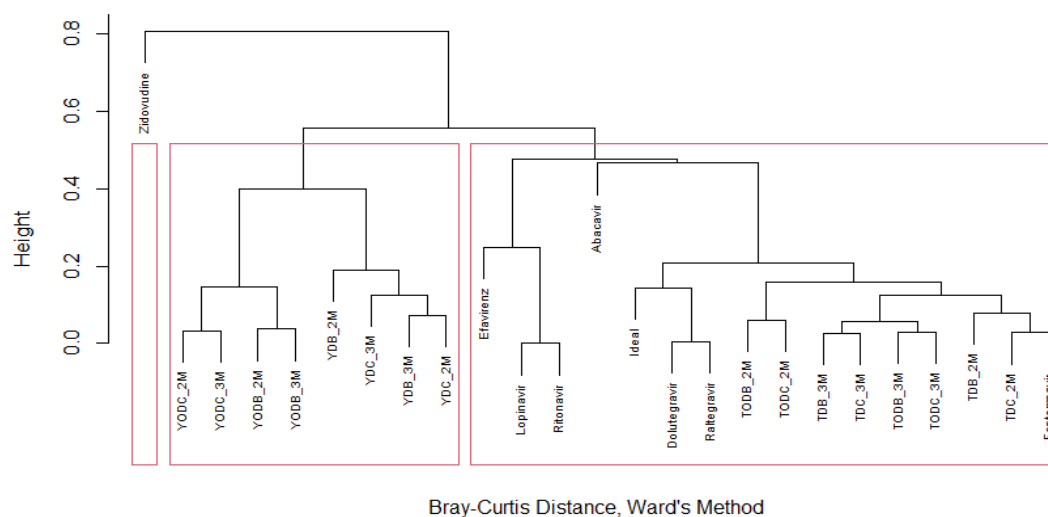
ADMET Predictor offers 5 individual models corresponding to enzymes used to diagnose hepatotoxicity. Possible elevation of alkaline phosphatase (ALP) was predicted only with YDC-3M, while all tertiary amines presenting bromine in their structure showed possible elevation of gamma-glutamyl transferase (GGT). On the other hand, the tyramines YDC-2M, YDC-3M, YODB-2M, and YODB-3M showed possible elevation of lactate dehydrogenase (LDH). No compound predicted elevation of Aspartate Aminotransferase (SGOT) or Alanine Aminotransferase (SGPT) enzymes. In contrast, zidovudine, ritonavir, and lopinavir showed significant potential to cause liver damage by elevation of ALP, LDH, GGT, and SGPT.

In terms of accumulated toxicity, none of the compounds or controls exhibited high toxicity. Low toxicity was observed for L-tyrosine derivatives, except for TODB-2M, and medium toxicity for tyramines, except for compounds YODC-2M and YODC-3M, which present low toxicity. The compound predicted to be the most toxic in the toxicity parameters evaluated was YDB-2M (7 points), like the control drugs efavirenz and zidovudine (8 points).

In addition, *Table 4* shows the data corresponding to the global risks (ADMET-Risk) calculated by the software, where the rules of Lipinski are considered. In this case, all compounds have a minimum global risk since they presented a score of less than 7, except for the control drugs lopinavir and ritonavir, with scores of 7.5 and 9.7, respectively.

In complement to the parameters described in *Table 4*, with the additional results of biological activity of the ADMET predictor, a hierarchical cluster analysis (Ward's method, Bray-Curtis similarity index) was performed with R, where the formation of three clusters was observed (*Figure 3*). In this case, the most promising compounds in terms of toxicity are those in the same group as the "ideal" compound, which, as seen in the dendrogram, are the L-tyrosine derivatives and the control drugs dolutegravir, raltegravir and fostemsavir, which have the lowest cumulative toxicity. In the second cluster are placed all tyramine derivatives, which were more toxic than L-tyrosine derivatives, with cumulative toxicity in the range of 4-7 points. Finally, zidovudine occupied the third cluster, with major differences with respect to the other compounds in terms of toxicity level.

Figure 3. Cluster analysis of di-halogenated compounds. Hierarchical cluster analysis (Ward's



method, Bray-Curtis similarity index) based on the toxicity parameters of the different compounds, evaluated by ADMET predictor®.

Anti-HIV-1 BaL (R5 strain) *in vitro* activity screening of di-halogenated compounds

As a strategy for determining the antiviral effect of the compounds, an antiviral screen was performed on TZM-bl cells, which were infected with HIV-1 BaL, using Gag p24 at 2 ng/ml.

The L-tyrosine-derived brominated compounds with free phenolic OH TDB-2M and TDB-3M showed no anti-HIV-1 activity at any of the concentrations tested. In contrast, replication seems to be promoted compared to positive infection control (*Figure 4A – B and Supplementary table 1*). The analogues chlorinated TDC-2M (IC₅₀ 140.7 μM) and TDC-3M, statistically significantly ($p < 0.0001$) inhibited HIV-1 BaL infection by 47.3% (300 μM) and 39.7% (75 μM), respectively, compared to the positive infection control, as shown in *Figure 4C – D and Supplementary table 1*.

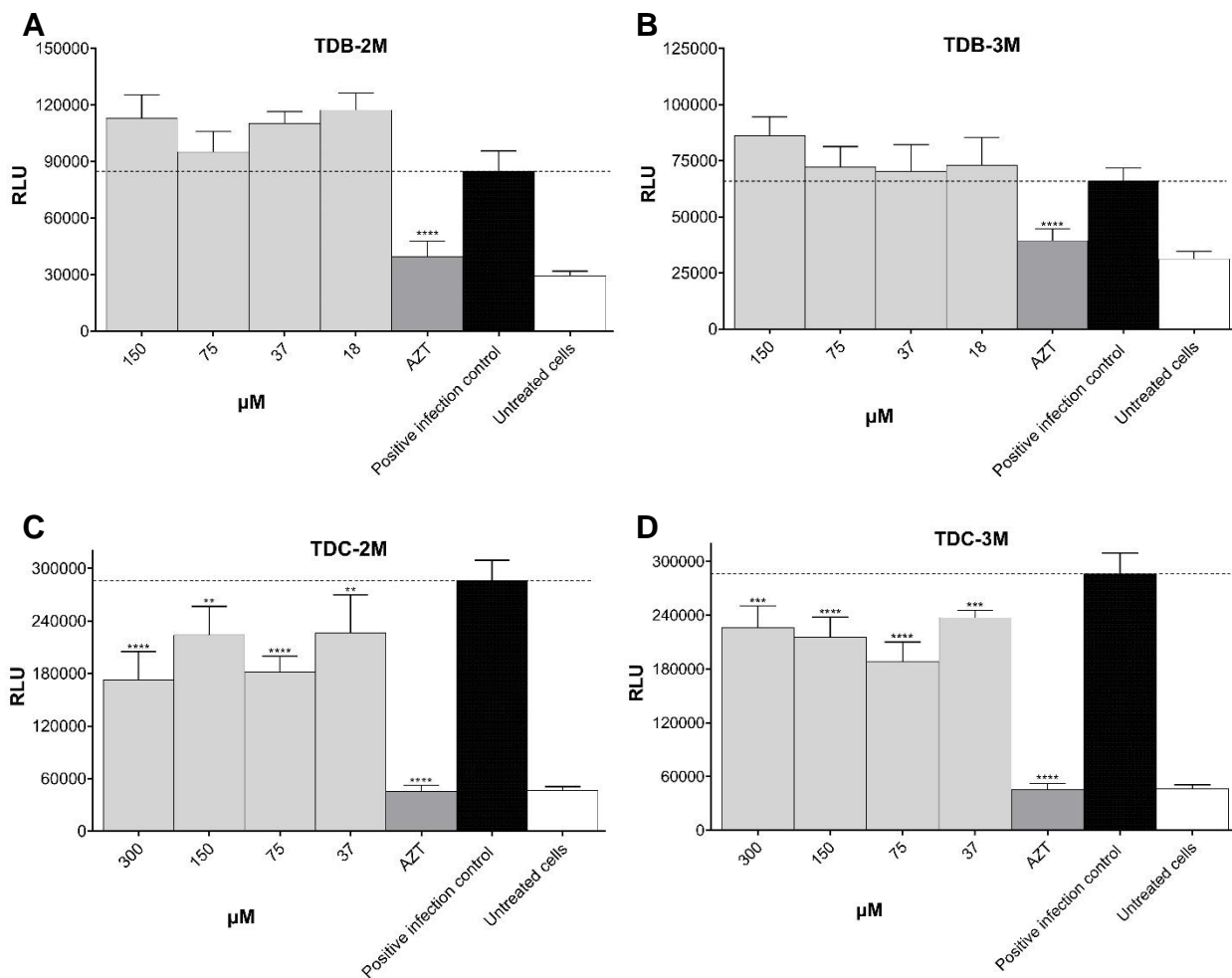


Figure 4. Antiviral activity of di-halogenated L-tyrosine-derived compounds with free phenolic OH on HIV-1 BaL replication. A. TDB-2M B. TDB-3M C. TDC-2M D. TDC-3M. AZT (10 μM) was used as a control of replication inhibition. Each sample was tested in triplicate in two independent experiments; the results have shown as mean ± standard deviation. The signs **, *** and **** above the columns mean $p > 0.01$, $p < 0.001$ and $p < 0.0001$, respectively, and correspond to the comparison with the positive infection control. The dotted line indicates the RLU of the positive infection control.

The compound TODB-2M (IC₅₀ 113.5 μM) at a concentration of 150 μM showed an anti-HIV activity of 45.8%, which was statistically significant (p<0.0001). In contrast, its respective quaternary ammonium salt (TODB-3M) showed no antiviral activity (*Figure 5A - B and Supplementary table 1*). On the other hand, the analogs chlorinated TODC-2M (IC₅₀ 67.42 μM) and TODC-3M (IC₅₀ 333.5 μM) inhibited HIV-1 BaL infection statistically significantly (p<0.0001) by 61.1% (150 μM) and 59.9% (300 μM), respectively (*Figure 5C - D and Supplementary table 1*).

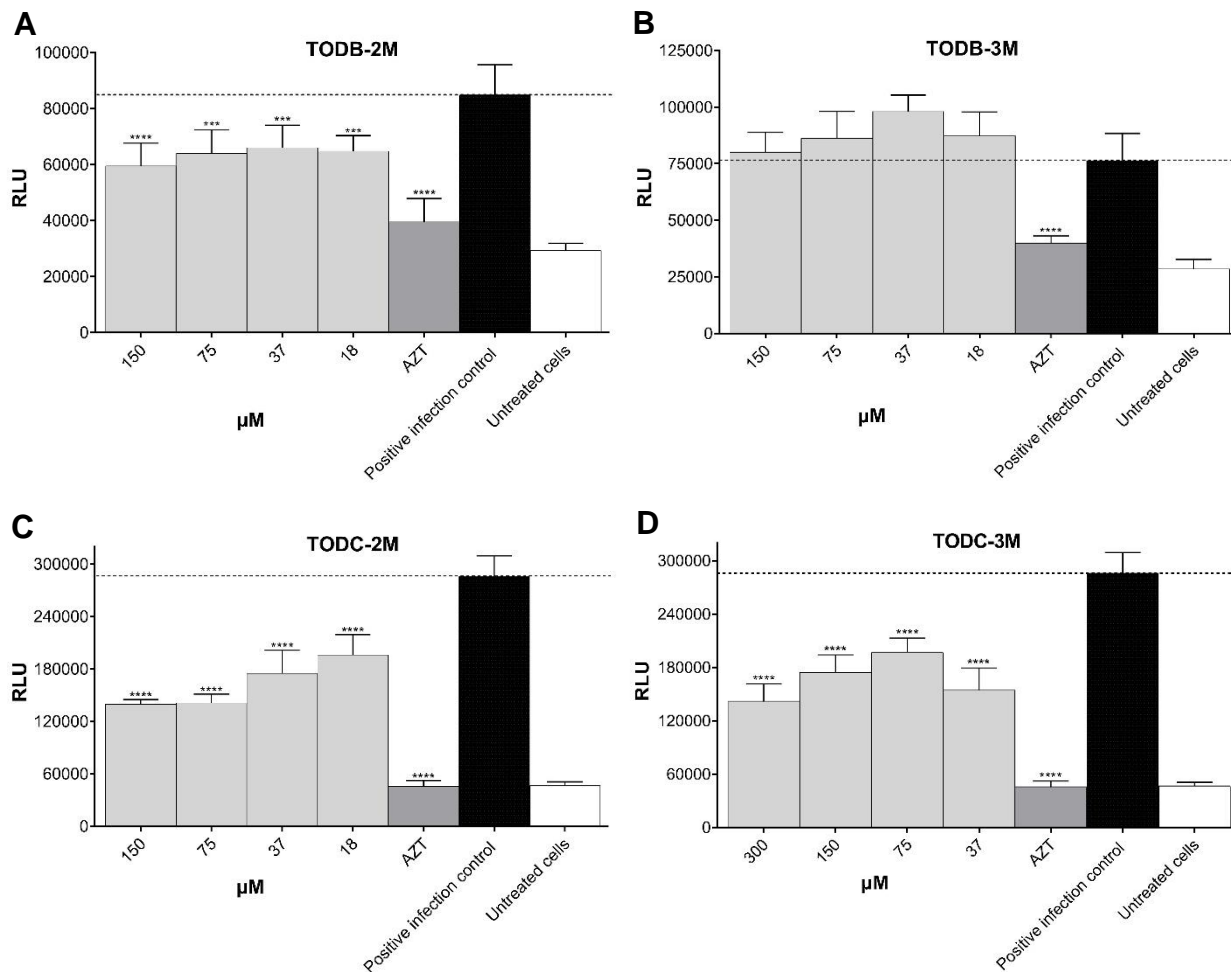


Figure 5. Antiviral activity of di-halogenated methyl ether L-tyrosine-derived compounds on HIV-1 BaL replication. Antiviral activity was assessed by luminescence. **A.** TODB-2M **B.** TODB-3M **C.** TODC-2M **D.** TODC-3M. AZT (10 μM) was used as a control. Each sample was tested in triplicate in two independent experiments; the results have shown as mean ± standard deviation. The signs *** and **** above the columns mean p<0.001 and p<0.0001, respectively,

and correspond to the comparison with the positive infection control. The dotted line indicates the RLU of the positive infection control.

The tyramine-derived brominated compounds YDB-2M and YDB-3M showed no statistically significant anti-HIV-1 activity. On the other hand, at the highest concentration tested, both compounds increased viral replication concerning the positive infection control, as shown in *Figures 6A – B and Supplementary table 1*. It was statistically significant (p 0.0045 and $p < 0.0001$, respectively). The analogue chlorinated YDC-2M did not inhibit HIV-1 BaL replication statistically significantly. In comparison to its respective quaternary ammonium salt YDC-3M (IC_{50} 37.2 μ M), which inhibited the infection by 50.2% (18 μ M) in a statistically significant manner ($p < 0.0001$), YDC-3M activity was inversely proportional to the concentrations used, as seen in *Figure 6C - D and Supplementary table 1*.

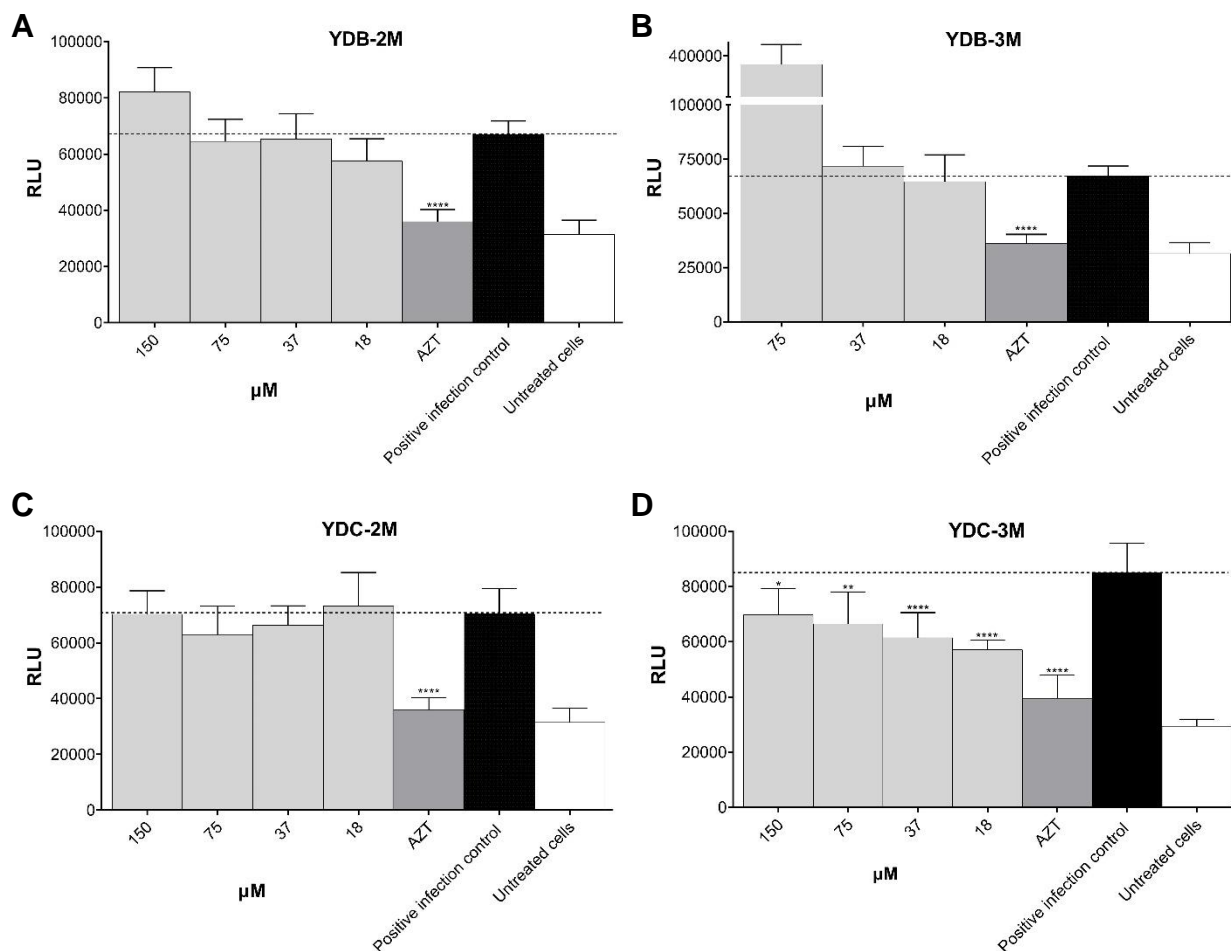


Figure 6. Antiviral activity of di-halogenated L-tyrosine-derived compounds with free phenolic OH on HIV-1 BaL replication. Antiviral activity was assessed by luminescence. **A.**

YDB-2M **B**. YDB-3M **C**. YDC-2M **D**. YDC-3M. AZT (10 μ M) was used as a control. Each sample was tested in triplicate in two independent experiments; the results have shown as mean \pm standard deviation. The signs *, ** and **** above the columns mean $p < 0.05$, $p < 0.01$ and $p < 0.0001$, respectively, and correspond to the comparison with the positive infection control. The dotted line indicates the RLU of the positive infection control.

Although the brominated compound YODB-2M had no antiviral effect at any of the concentrations tested, it increased viral replication statistically ($p = 0.0031$) at a concentration of 75 μ M. Similarly, the quaternary ammonium salt YODB-3M demonstrated the same effect but at a concentration of 18 μ M. Also, the chlorinated compounds YODC-2M and YODC-3M did not show any antiviral activity compared to the positive infection control, as illustrated in *Figure 7A - D and Supplementary table 1*. Finally, the positive inhibition control (AZT) at a concentration of 10 μ M inhibited more than 90% of virus infection in TZM-bl cells. The inhibition percentages of each compound at the different concentrations evaluated are shown in *Supplementary table 1*.

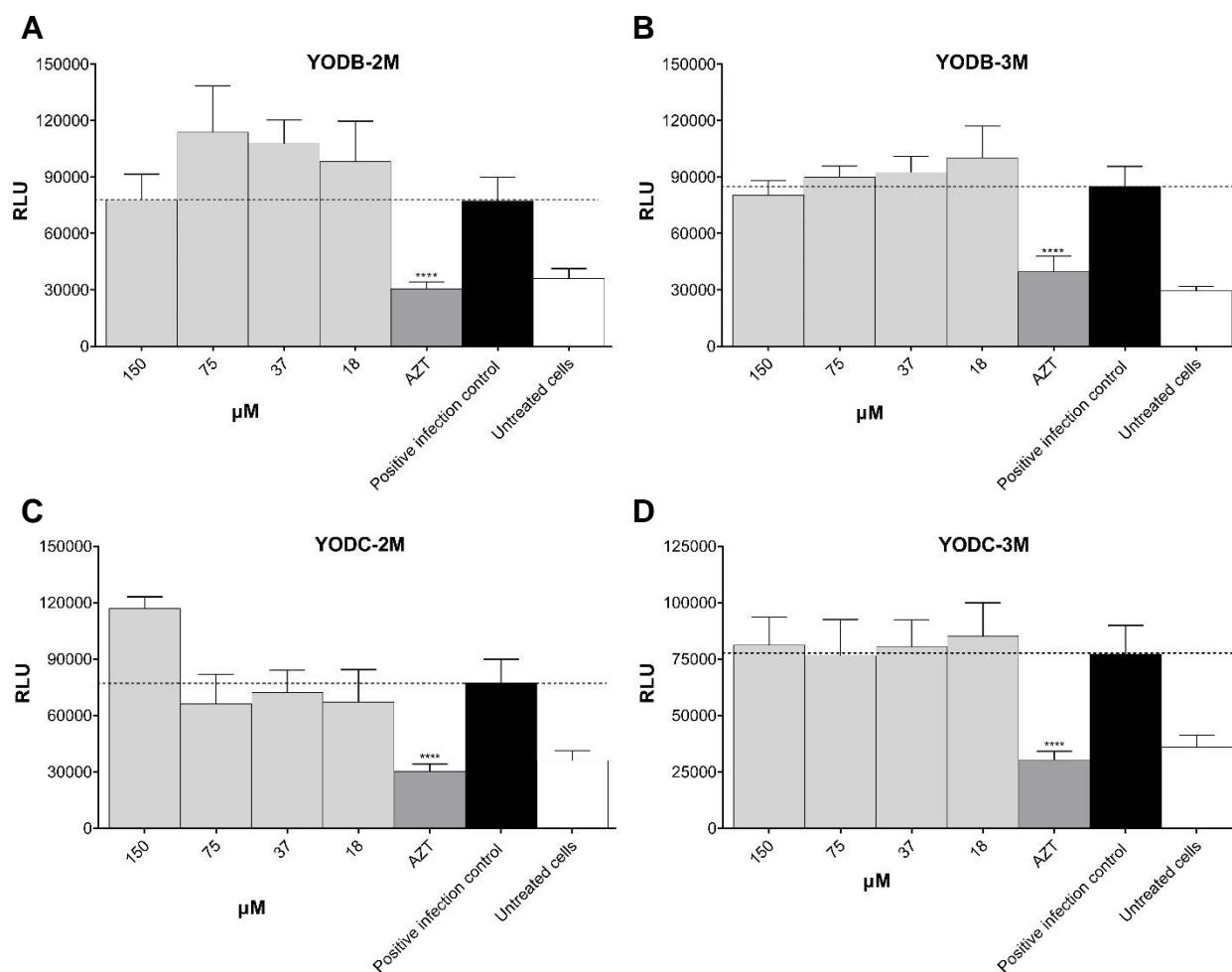


Figure 7. Antiviral activity of di-halogenated methyl ether tyramine-derived compounds on HIV-1 BaL replication. Antiviral activity was assessed by luminescence. **A.** YODB-2M **B.** YODB-3M **C.** YODC-2M **D.** YODC-3M. AZT (10 μM) was used as a control. Each sample was tested in triplicate in two independent experiments; the results have shown as mean ± standard deviation. The sign **** above the columns mean p<0.0001 and corresponds to the comparison with the positive infection control. The dotted line indicates the RLU of the positive infection control.

Compounds TDC-2M, TODB-2M, TODC-2M, TODC-3M and YDC-3M, which were active against R5 strain, showed a SI of ~1.24, 1.45, >4.45, 0.22 and 1.07, respectively (Table 5).

Compound	CC ₅₀ (μM)	CI ₅₀ (μM)	SI
TDC-2M	~ 174,4	140,7	~1.24
TDC-3M	>300	-	-
TODB-2M	164,9	113,5	1.45

TODC-2M	>300	67,42	>4.45
TODC-3M	74,9	333,5	0.22
YDC-3M	39,88	37,7	1.07

Table 5. Selectivity index of the compounds against HIV-1 BaL.

When it was compared the number of times in which the concentration of the compounds differed from those of the Inhibition control (AZT= 10 μ M), we observed that for TDC-2M this was 30 times higher. Similarly, compared with the compounds TODC-3M, TODB-2M, TODC-2M, and YDC-3M, the concentration was also 30, 15, 15 and 1.8 times higher than AZT concentration, respectively.

Anti- HIV-1_{III}B (X4 strain) *in vitro* activity screening of di-halogenated compounds

Similarly, antiviral screening was performed on TZM-bl cells that were infected with HIV-1_{III}B (X4 strain) using a Gag p24 concentration of 10 ng/ml.

The brominate L-tyrosine-derived with free phenolic OH compounds TDB-2M and TDB-3M did not inhibit HIV-1 replication compared to the positive infection control (*Figures 8A – B and Supplementary table 2*). The analogue chlorinated TDC-2M no-showed activity against HIV-1 at any of the concentrations tested. Instead, it significantly promoted infection ($p < 0.0001$) at a concentration of 150 μ M. The respective quaternary ammonium salt TDC-3M did not inhibit HIV-1 infection statistically significantly compared to the positive infection control (*Figure 8C – D and Supplementary table 2*).

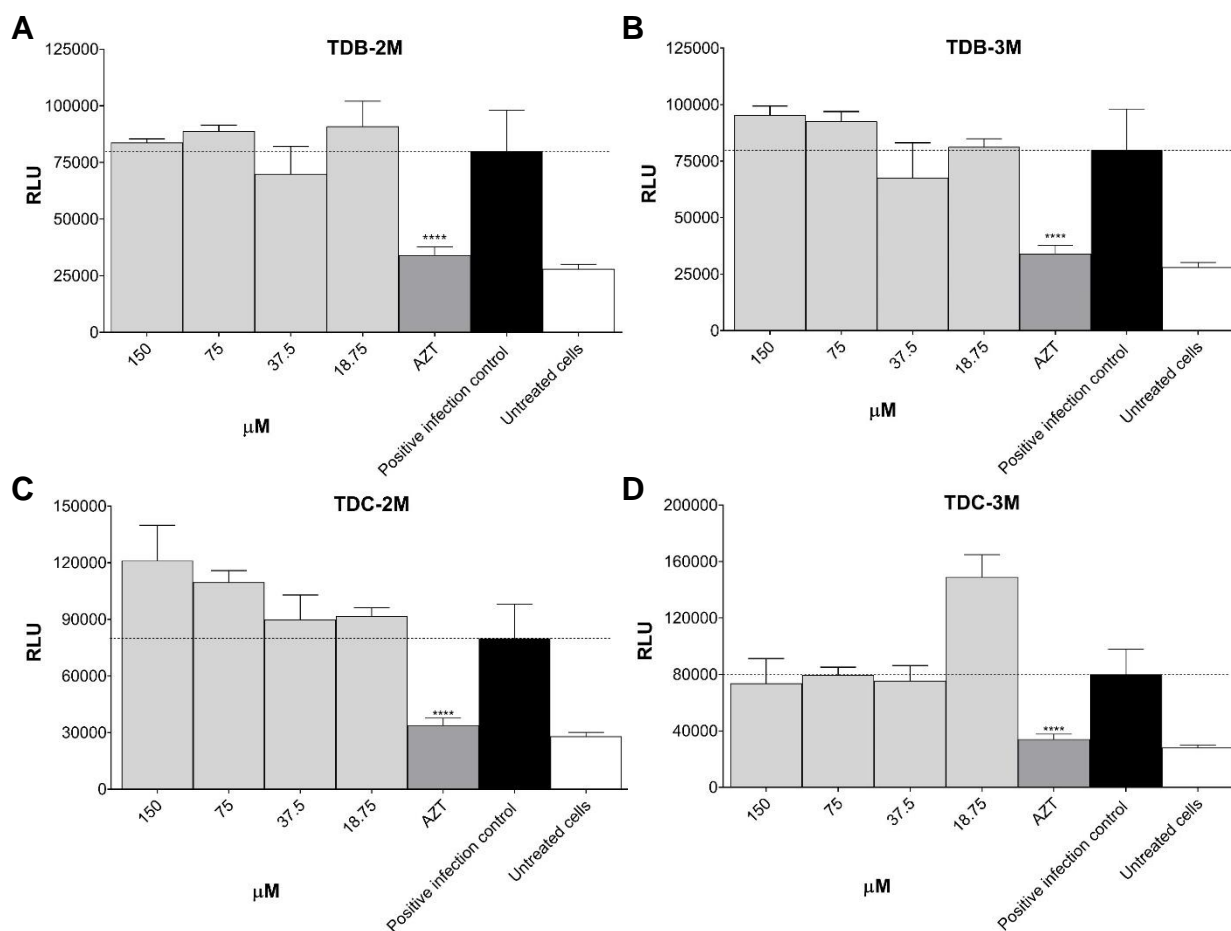


Figure 8. Antiviral activity of di-halogenated L-tyrosine-derived compounds with free phenolic OH on HIV-1_M replication. Antiviral activity was assessed by luminescence. **A.** TDB-2M **B.** TDB-3M **C.** TDC-2M **D.** TDC-3M. AZT (10 μM) was used as a control. Each sample was tested in triplicate in two independent experiments; the results have shown as mean ± standard deviation. The sign **** above the columns mean $p < 0.0001$ and corresponds to the comparison with the positive infection control. The dotted line indicates the RLU of the positive infection control.

The brominated tertiary amine TODB-2M ($IC_{50} \sim 82.68 \mu M$) showed potent antiviral activity with an inhibition percentage of 95.9% (150 μM), with statistically significant differences ($p < 0.0001$) compared to the positive infection control (*Figure 9A and Supplementary table 2*). On the other hand, the respective quaternary ammonium salt TODB-3M no-showed statistically significant inhibitory activity (*Figure 9B*). Similar results were observed with the chlorinated compounds; TODC-2M ($IC_{50} \sim 39.15 \mu M$) showed a statistically significant ($p < 0.0001$) antiviral activity of 99.6% (150 μM), while the inhibition presented by TODC-3M was not statistically significant (*Figures 9C – D and Supplementary table 2*).

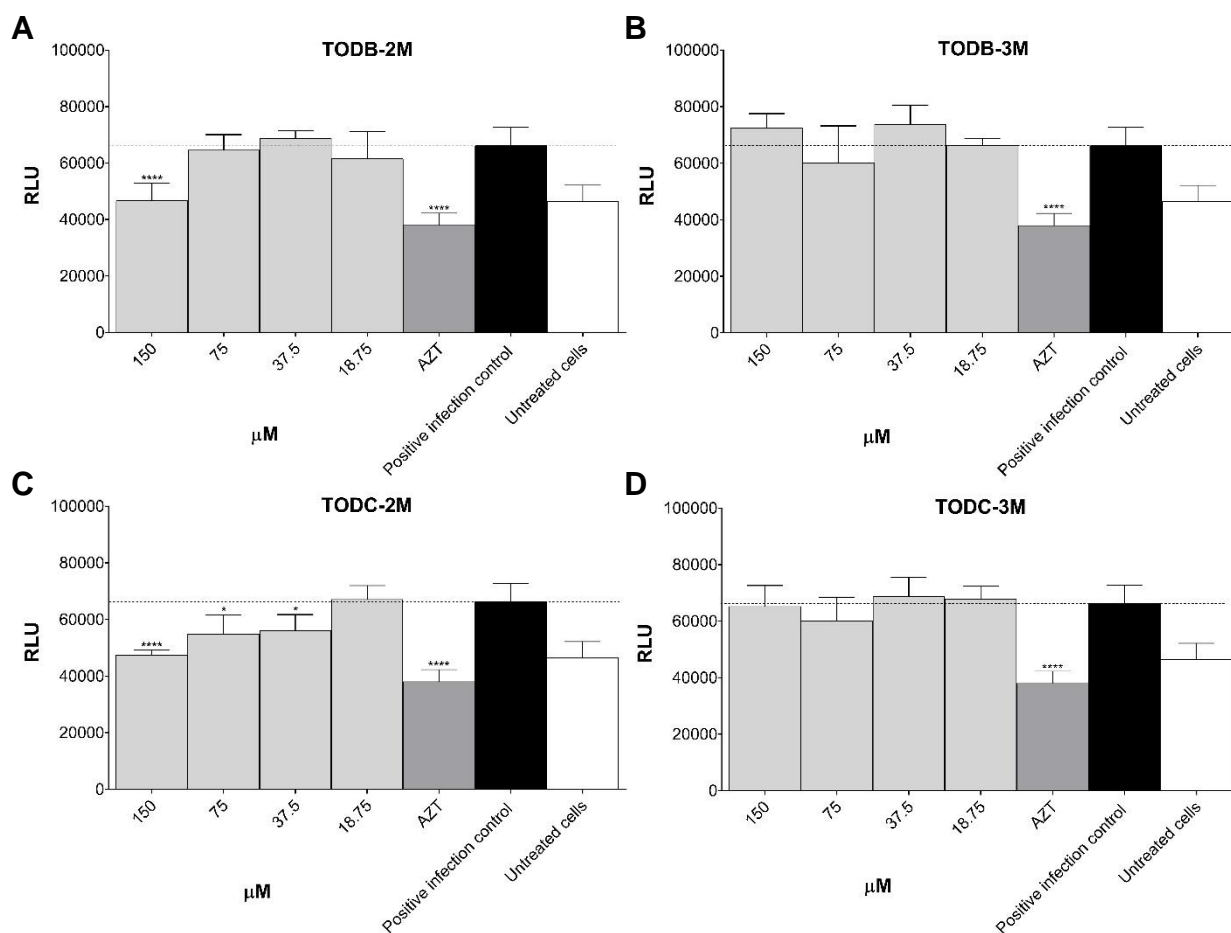


Figure 9. Antiviral activity of di-halogenated methyl ether L-tyrosine-derived compounds on HIV-1_{MB} (X4 strain) replication. Antiviral activity was assessed by luminescence. **A.** TODB-2M **B.** TODB-3M **C.** TODC-2M **D.** TODC-3M. AZT (10 μM) was used as a control. Each sample was tested in triplicate in two independent experiments; the results have shown as mean ± standard deviation. The signs * and **** above the columns mean $p < 0.05$ and $p < 0.0001$, respectively, and correspond to the comparison with the positive infection control. The dotted line indicates the RLU of the positive infection control.

The tyramine-derived compounds YDB-2M and YDC-2M did not inhibit HIV-1 infection a statistically significantly compared to the positive infection control, as seen in *Figure 10A, C*. In contrast, the respective quaternary ammonium salts YDB-3M (IC₅₀ 3.090 μM) and YDC-3M (IC₅₀ 22.31 μM) at a concentration of 18 μM inhibited HIV-1 replication by 39.2% and 40.9%, respectively, with statistically significant differences ($p < 0.0001$) compared to the positive infection control (*Figures 10B, D and Supplementary table 2*).

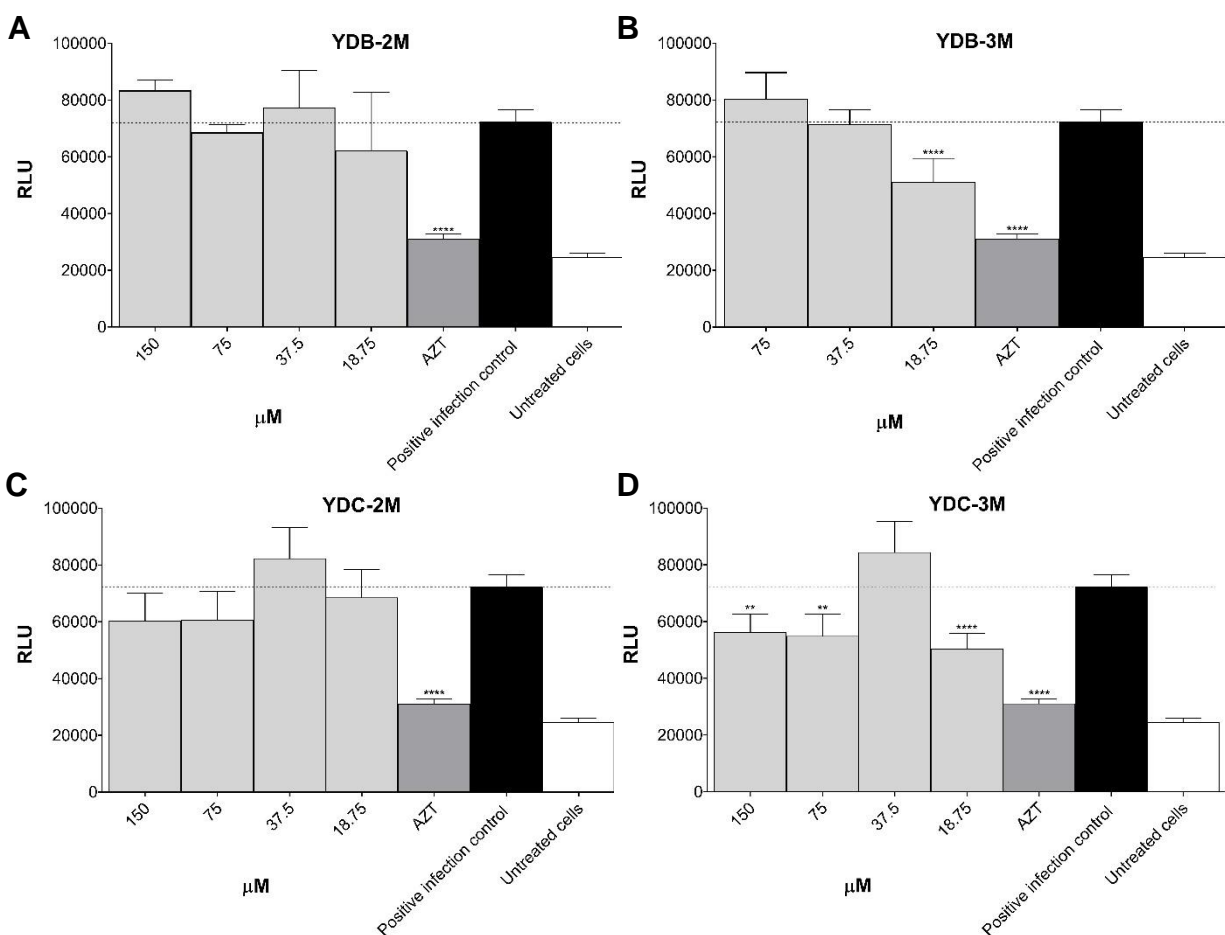


Figure 10. Antiviral activity of di-halogenated L-tyrosine-derived compounds with free phenolic OH on HIV-1_{IIIB} (X4 strain) replication. Antiviral activity was assessed by luminescence. **A.** YDB-2M **B.** YDB-3M **C.** YDC-2M **D.** YDC-3M. AZT (10 μM) was used as a control. Each sample was tested in triplicate in two independent experiments; the results have shown as mean ± standard deviation. The signs ** and **** above the columns mean p<0.01 and p<0.0001, respectively, and correspond to the comparison with the positive infection control. The dotted line indicates the RLU of the positive infection control.

Regarding the tyramine-derivates compounds with free phenolic OH, antiviral activity was only observed for YODB-3M (IC₅₀ 321.7 μM) with a percentage of inhibition of 20.3% (75 μM) in a statistically significant way (p=0.0004); the other compounds did not show antiviral activity (Figure 11 and Supplementary table 2). Finally, the positive inhibition control AZT at a concentration of 10 μM inhibited more than 90% of virus infections in TZM-bl cells. The inhibition percentages of each compound at the different concentrations evaluated are shown in Supplementary table 2.

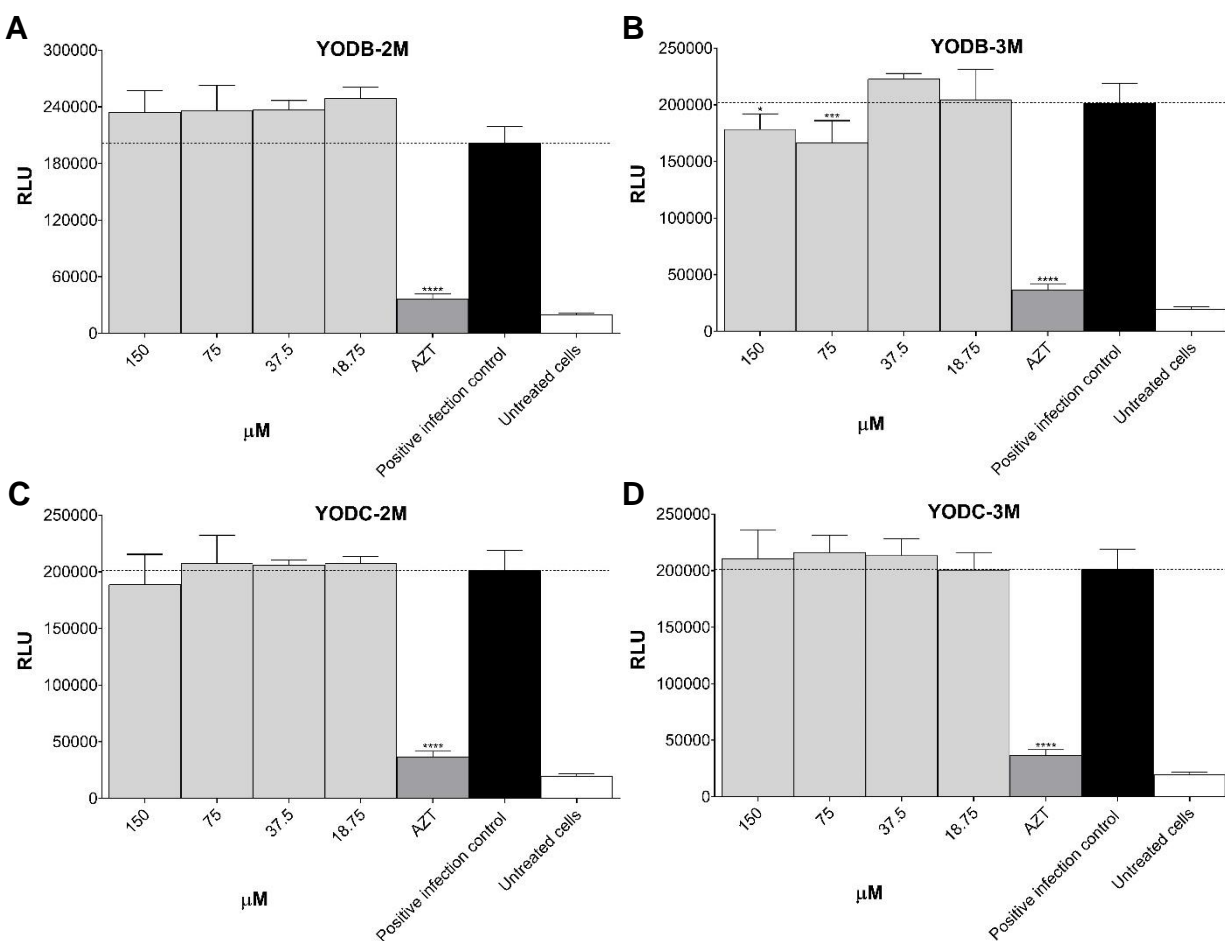


Figure 11. Antiviral activity of di-halogenated methyl ether tyramine-derived compounds on HIV-1_{IIIB} (X4 strain) replication. Antiviral activity was assessed by luminescence. **A.** YODB-2M **B.** YODB-3M **C.** YODC-2M **D.** YODC-3M. AZT (10μM) was used as a control. Each sample was tested in triplicate in two independent experiments; the results have shown as mean ± standard deviation. The signs *, ***, and **** above the columns mean $p < 0.05$, $p < 0.001$ and $p < 0.0001$, respectively, and correspond to the comparison with the positive infection control. The dotted line indicates the RLU of the positive infection control.

Compounds TODB-2M, TODC-2M, YDB-3M, YDC-3M and YODB-3M, which were active against X4 strain, showed a SI of ~1.99, ~7.66, 1.79, ~0.03 and 0.25, respectively (Table 6).

Compound	CC ₅₀ (μM)	CI ₅₀ (μM)	SI
TODB-2M	164,9	~82,68	~1.99
TODC-2M	>300	~39,15	~7.66
YDB-3M	~100,9	3.090	1.79

YDC-3M	39,88	22,31	~0.03
YODB-3M	78,7	321,7	0.25

Table 6. Selectivity index of the compounds against HIV-1_{III_B}.

In addition, we observed that the concentration of the compounds TODB-2M, TODC-2M, YDB-3M, YDC-3M y YODB-3M were 15, 15, 1.8, 1.8, and 7.5 times higher than AZT concentration, respectively.

Anti-HIV-GFP-VSV-G *in vitro* activity of di-halogenated compounds

According to the results obtained in the antiviral screening of the 16 compounds, the three compounds with the highest antiviral activity against both viral strains (R5 and X4) were chosen to evaluate the anti-HIV activity in a different viral model. These were TODB-2M, TODC-2M, and YDC-3M. Since viruses with CCR5 tropism (R5 strain) are responsible for the initial or acute HIV-1 infection, the TODC-3M compound was also chosen for this assay, since it obtained an inhibition percentage of 59.9% against the R5 strain.

The virus used for this assay was pseudotyped virus (HIV-GFP-VSV-G), which was produced by the transfection of HEK293T cells (*Figure 12*).

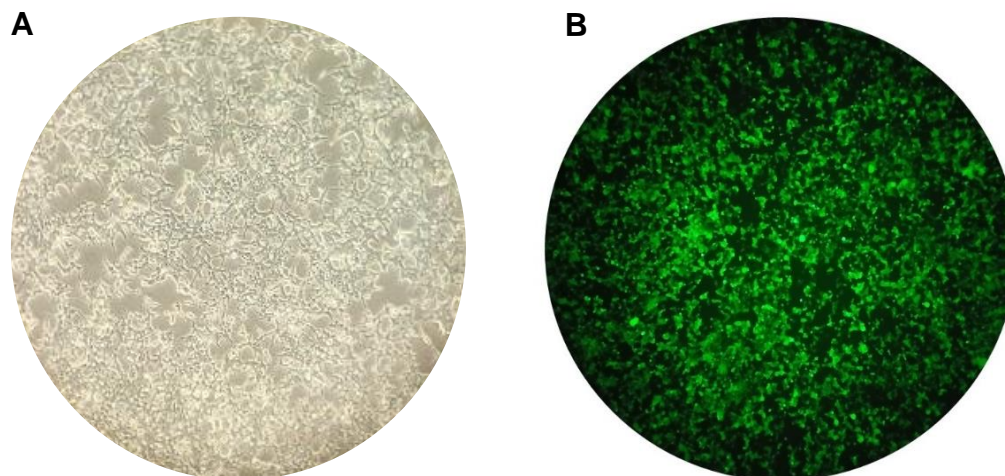


Figure 12. GFP expression in HEK293T cells co-transfected with HIV Δ env.GFP and pVSV-G plasmids. **A.** Cells observed in phase contrast bright field microscopy. **B.** Cells observed using the GFP filter cube. Cells were observed using a 10-fold objective lens.

TZM-bl cells were infected with 40 ng/ml of HIV-GFP-VSV-G and treated with the compounds, or AZT as an inhibition control of viral replication. The antiviral activity was measured after 48hrs

of infection through the evaluation of the percentage of GFP⁺ cells by flow cytometry. The representative gating strategy of the flow cytometry analysis is shown in *Figure 13*.

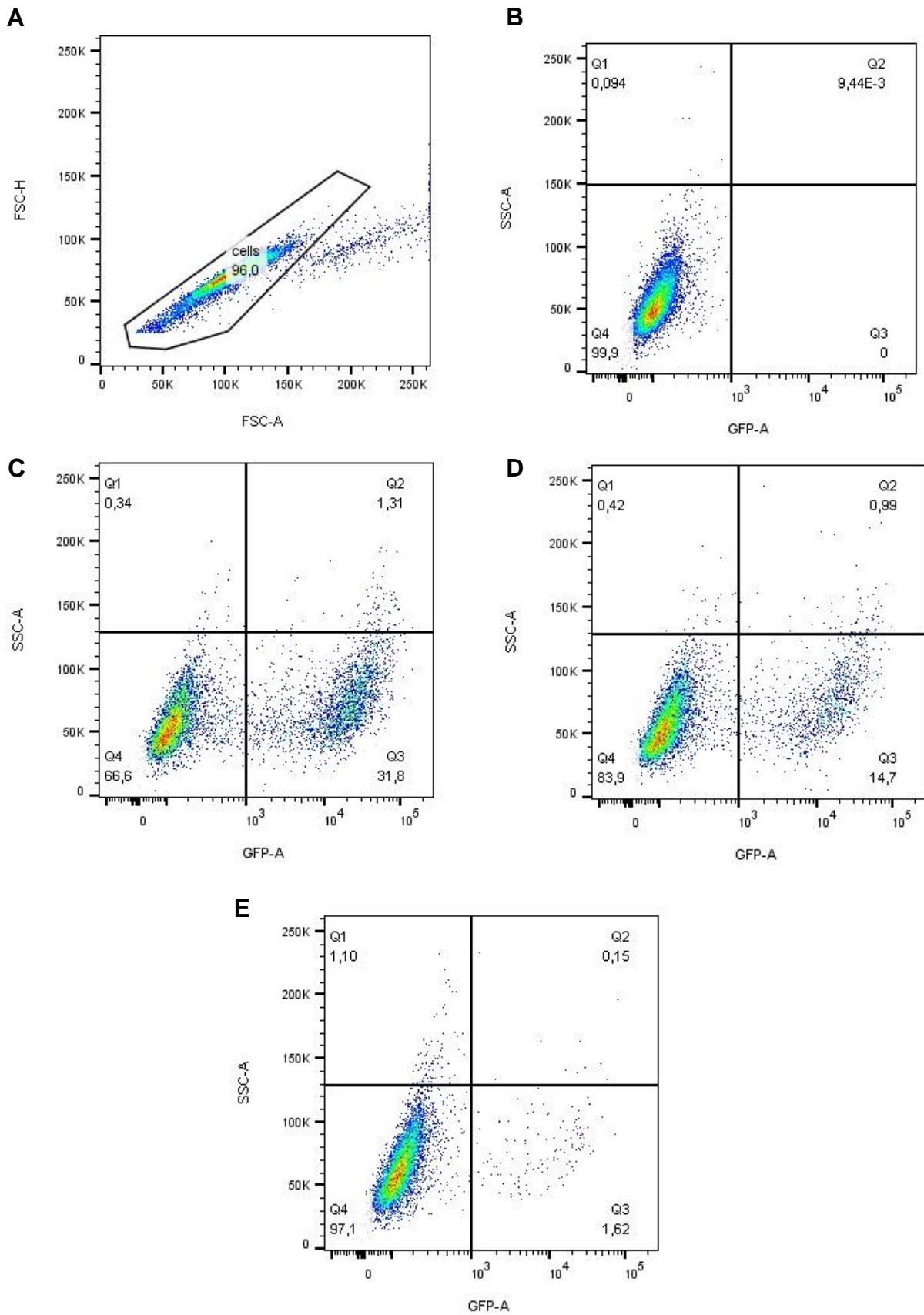


Figure 13. Representative flow cytometry gating strategy of TzM-bl GFP+ cells assessed 48 hours

post-infection. **A.** Population of TZM-bl cells. **B.** Percentage of GFP+ in uninfected TZM-bl cells. **C.** Percentage of GFP+ in TZM-bl cells infected with 40ng/ml of untreated p24. **D.** Percentage of GFP+ in TZM-bl cells infected with 40ng/ml p24 and treated with 150 μ M TODB-2M. **E.** Percentage of GFP+ in TZM-bl cells infected with 40ng/ml p24 and treated with 10 μ M AZT.

The tested compounds TODB-2M (IC₅₀ 141,8 μ M), TODC-2M (IC₅₀ 397,1 μ M), and YDC-3M (IC₅₀ 2784 μ M) showed a percentage inhibition of 44.2%, 29%, and 12.5%, respectively, at the highest concentration tested (150 μ M). These differences were statistically significant (p=0,0044, p=0,0184 and p=0,0138) for all compounds compared to the infection control. All three compounds inhibited HIV-1 replication in a dose-dependent manner. Compound TODC-3M inhibited infection by 19.5%, but it was not significantly different from the infection control. The positive inhibitory control, AZT, inhibited 93.2% of viral replication (*Figure 14*).

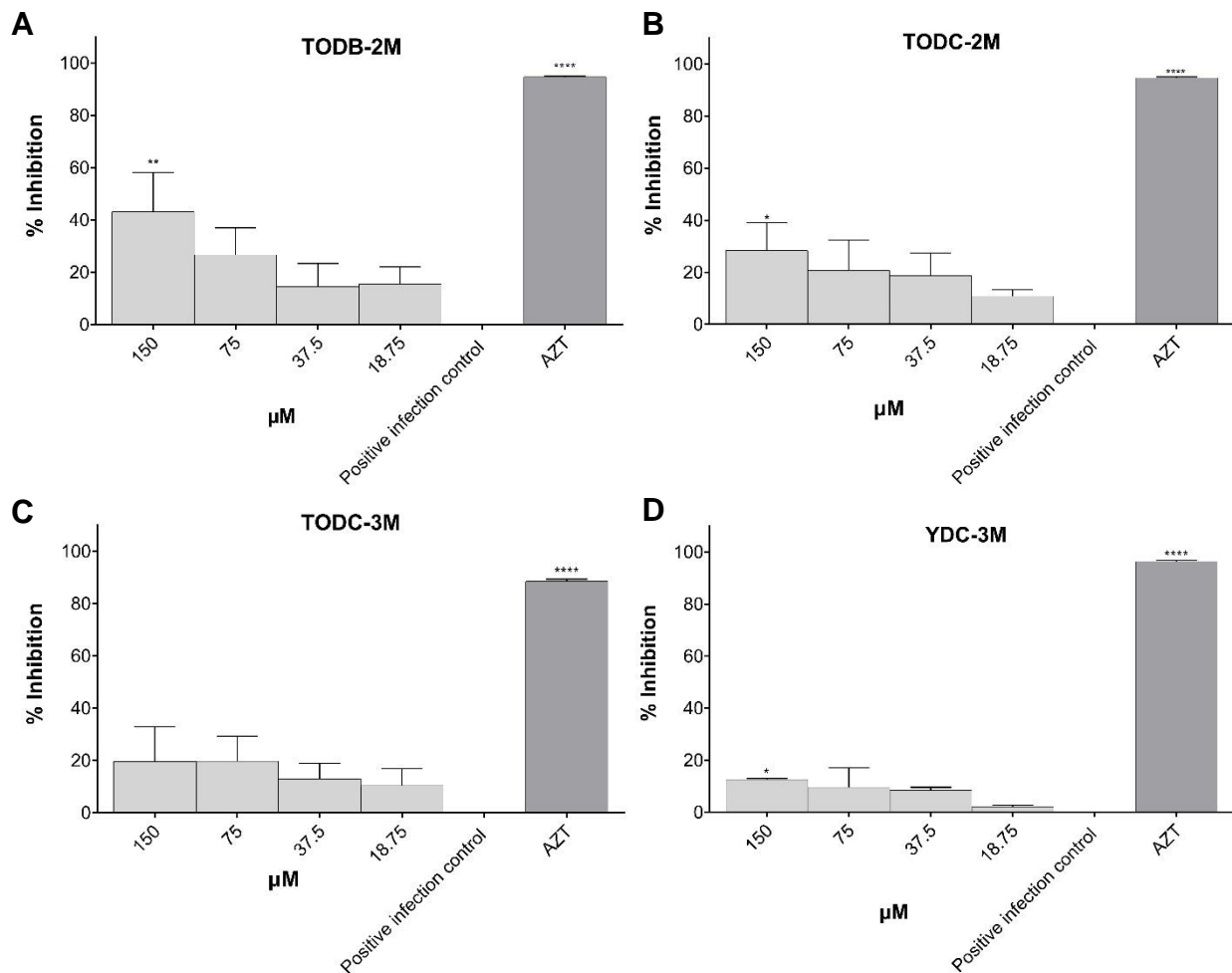


Figure 14. Antiviral activity of di-halogenated compounds on HIV-GFP-VSV-G *in vitro* replication. Antiviral activity was assessed by flow cytometry. **A.** TODB-2M **B.** TODC-2M **C.**

TODC-M D. YDC-3M. AZT (10 μ M) was used as a control of viral inhibition replication. The graphs represent the median of two independent experiments performed in triplicate but measured as a single pool; the results have shown as mean \pm standard deviation. The signs *, ** and **** above the columns mean $p < 0.05$ and $p < 0.01$ and $p < 0.0001$, respectively, and correspond to the comparison with the positive infection control.

Compounds TODB-2M, TODC-2M, and YDC-3M, which were active against pseudotyped virus obtained a selectivity index of 1.16, >0.75 , and 0.01, respectively (Table 7).

Compound	CC ₅₀ (μ M)	CI ₅₀ (μ M)	SI
TODB-2M	164,9	141,8	1.16
TODC-2M	>300	397,1	>0.75
YDC-3M	39,88	2784	~ 0.01

Table 7. Selectivity index of the compounds against HIV-GFP-VSV-G.

The concentration of the compounds TODB-2M, TODC-2M, and YDC-3M, were 15 times above the AZT concentration.

The L-tyrosine derivatives exhibit favorable binding energies with the tested proteins.

To evaluate the possible interaction of the compounds on viral proteins, *in silico* molecular docking of each compound with 7 of the HIV-1 viral proteins: gp120 (PDB: 4J6R), gp41 (PDB: 3VTQ), RT (PDB: 4G1Q), IN (PDB: 1QS4-3OYA), protease (PDB: 5YOK), p17 (PDB: 4JMU) and p24 (PDB: 2XDE) was evaluated.

All compounds had favorable binding energies against the different proteins evaluated (between -3.53 ± 0.047 and -9.37 ± 0.09 Kcal/mol). Still, the compounds only qualified the established threshold value ($\Delta G_{\text{bind}} = -6.0$ Kcal/mol) as a strong interaction when docked with protease and reverse transcriptase. Similarly, only the chlorinated tertiary amines (YDC-2M and YODC-2M) satisfied this threshold when interacting with gp120 (Supplementary table 3 and Figure 15).

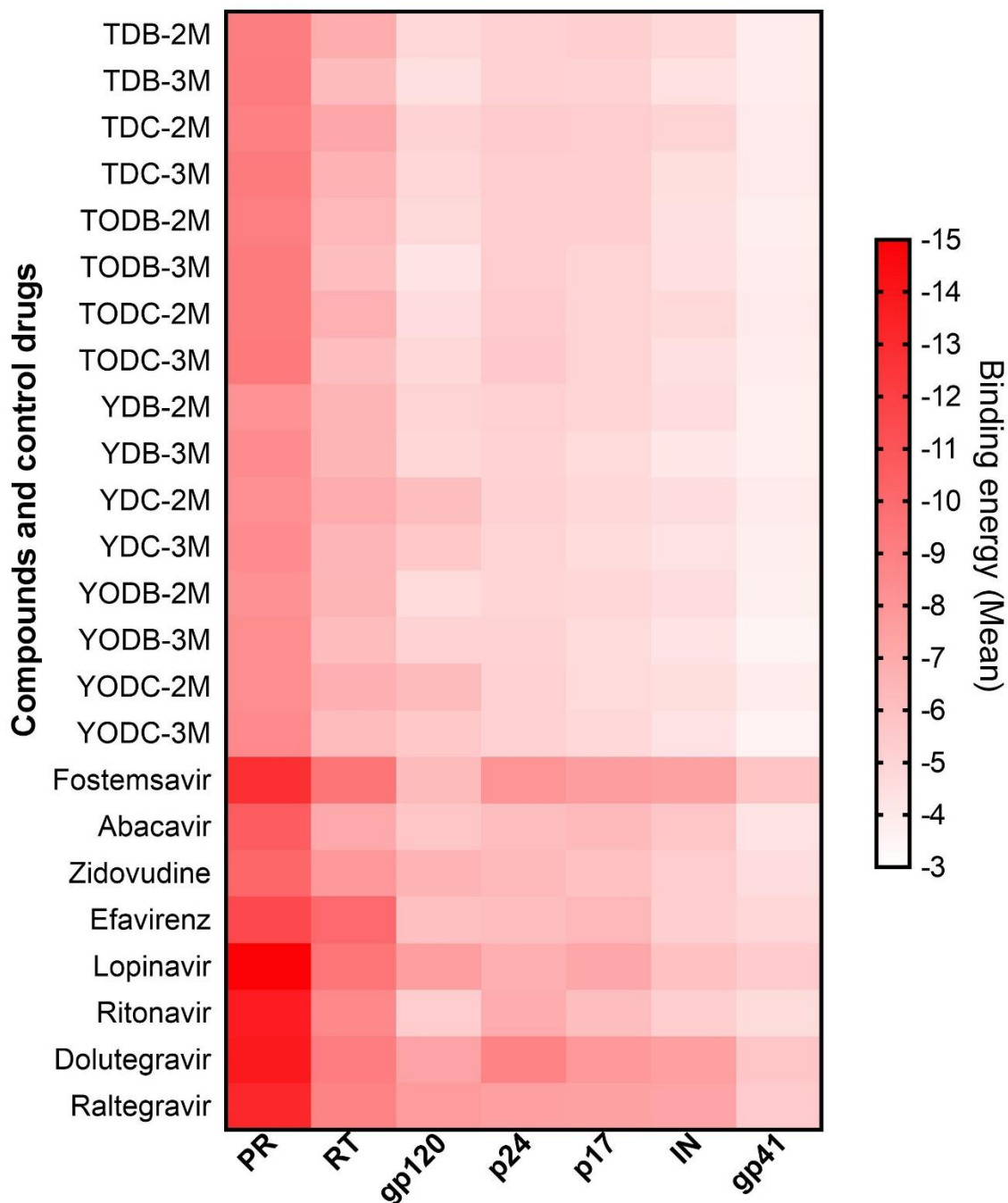
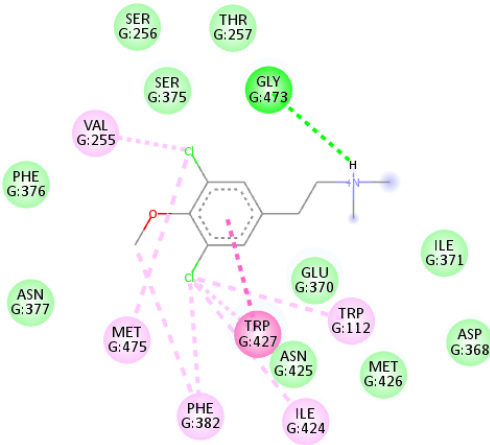
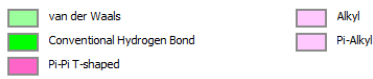
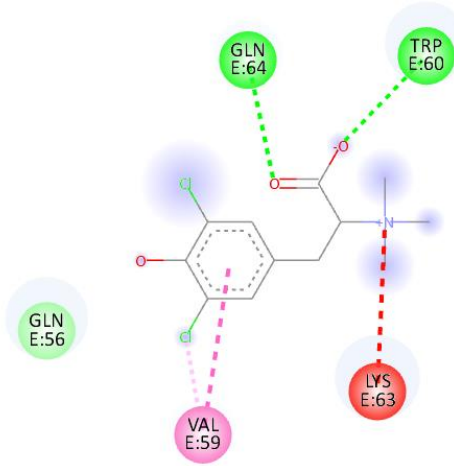
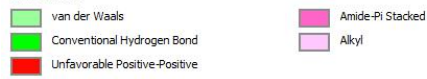
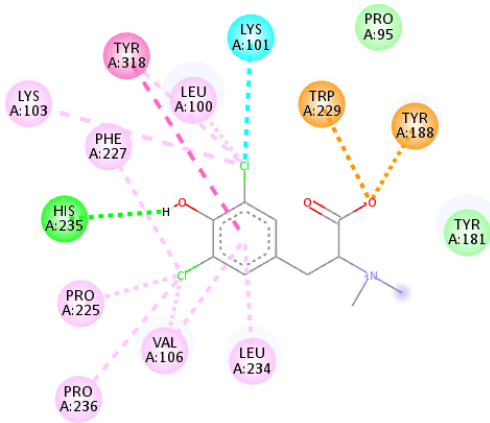
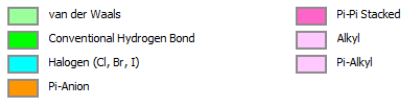
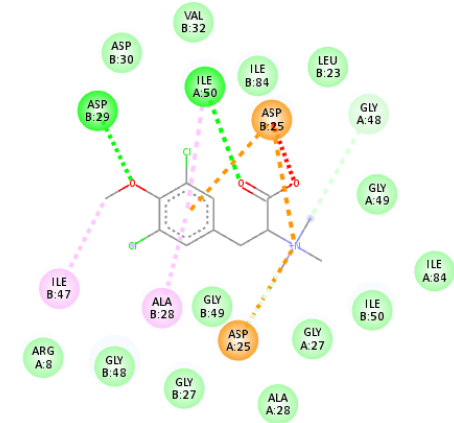
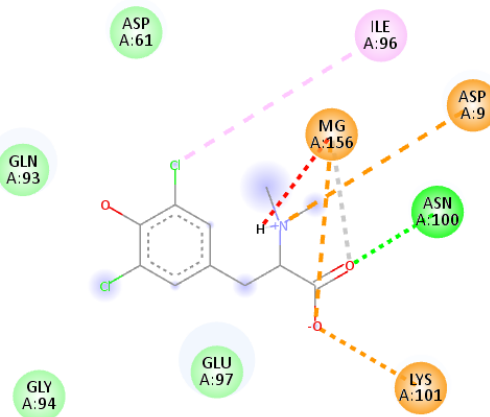
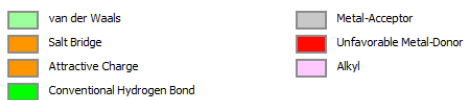
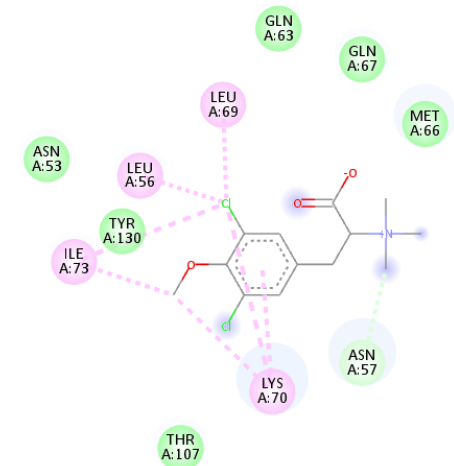
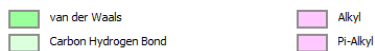


Figure 15. Heat map of binding energies between compounds and viral proteins and study control drugs. Free binding energies were obtained by molecular docking with AutodockVina®. Each interaction was analyzed in triplicate. Less than 0 kcal/mol were considered favorable energies. The averages were graphed in color scale red. PR (protease), RT (Reverse transcriptase), gp120 (glycoprotein 120), p24 (capsid protein), p17 (matrix protein), IN (integrase), gp41 (glycoprotein 41).

The free binding energies obtained between HIV-1 glycoprotein 120 (gp120) and the compounds ranged from -4.0 ± 0.0 to -6.23 ± 0.05 Kcal/mol (*Supplementary table 3 and Figure 15*). The approved control drug inhibiting this protein is fostemsavir (FTR), which obtained binding energy of -6.23 ± 0.40 Kcal/mol and formed hydrogen-bond interactions with Asn425, Gly431, and Gln432 and hydrophobic interactions with residues Thr257, Asp368, Glu370, Ile371, Met426, Trp427, Ala430, Gly473, and Met475. The compound that presented the most favorable binding energy (-6.23 ± 0.05 Kcal/mol) and complied with the established threshold value ($\Delta G_{\text{bind}} = -6.0$ Kcal/mol) was YODC-2M forming a hydrogen bond with Gly473 and Van der Waals, alkyl and pi – pi T interactions with the Trp112 residues, Val255, Ser256, Thr257, Asp368, Glu370, Ile371, Ser375, Phe376, Asn377, Phe382, Ile424, Asn425, Met426, Trp427 and Met475 (*Figure 16A*).

A**Interactions****B****Interactions****C****Interactions****D****Interactions****E****Interactions****F****Interactions**

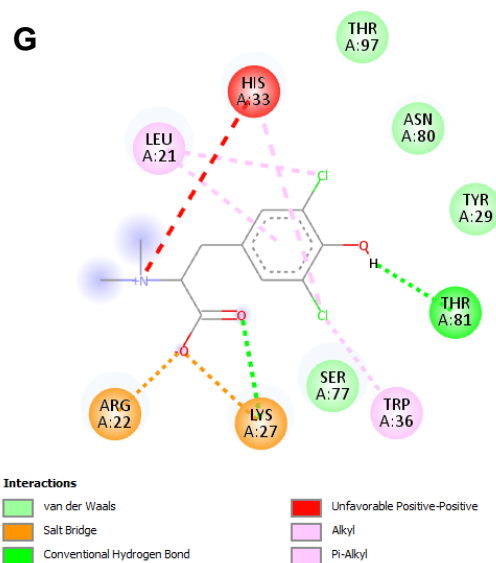


Figure 16. Compounds that obtained higher binding energy with the different viral proteins were evaluated in molecular docking. A) Interactions between gp120 and YODC-2M; B) gp41 and TDC-3M; C) RT and TDC-2M; D) PR and TODC-3M; E) IN and TDC-2M; F) p24 and TODC-3M; G) p17 and TDC-2M. The figures obtained using Discovery Studio show the possible docking site of the compounds on the viral proteins.

The interaction scores between HIV-1 glycoprotein 41 (gp41) and the compounds ranged from -3.53 ± 0.05 to $-4.0 \pm 0.0 \pm 0.0$ Kcal/mol (*Supplementary table 3 and Figure 15*). TDC-3M formed two hydrogen bonds with residues Trp60 and Gln64 and interacted with Gln56, and Val59, in addition an unfavorable interaction with Lys63 was obtained (*Figure 16B*).

The binding energies obtained between the reverse transcriptase (RT) and the compounds were between -6.03 ± 0.05 and -7.20 ± 0.00 Kcal/mol. All compounds complied with the established threshold value ($\Delta G_{\text{bind}} = -6.0$ Kcal/mol) (*Supplementary table 3 and Figure 15*). The control drug that obtained the strongest binding energy (-10.10 ± 0.00 Kcal/mol) was efavirenz (EFV) and interacted with residues Leu100, Lys101, Lys103, Val106, Val179, Tyr181, Tyr188, Gly190, Pro225, Phe227, Trp229, Leu234, His235, Pro236, Tyr318. The most favorable binding energy (-7.2 ± 0.0 Kcal/mol) was with TDC-2M via hydrogen bond formation with His235 and Van der

Waals interactions with Pro95, Leu100, Lys101, Lys103, Val106, Tyr181, Tyr188, Pro225, Phe227, Trp229, Leu234, Pro236 and Tyr318 (*Figure 16C*).

The interaction scores between HIV-1 protease and the compounds ranged from -8.17 ± 0.05 to -9.37 ± 0.09 Kcal/mol. All compounds complied with the established threshold value ($\Delta G_{\text{bind}} = -6.0$ Kcal/mol) (*Supplementary table 3 and Figure 15*). The control drug that obtained the strongest binding energy (-14.97 ± 0.05 Kcal/mol) was lopinavir (LPV) and interacted with residues Asp25, Asp25', Ile50, Ile50', Gly27, and Asp29, forming six hydrogen bonds, and with other residues of both chains, close to the active site by Van der Waals interactions. The compound that presented the most favorable binding energy (-9.37 ± 0.09 Kcal/mol) was TODC-3M forming two hydrogen bonds with Asp29', and Ile50, obtained attractive charges with residues Asp25 and Asp25' and Van der Waals interactions with other residues close to the active site. Moreover, this compound presented an unfavorable negative-negative interaction between the carboxyl group and Asp25' (*Figure 16D*).

The binding energies obtained between the integrase (IN) and the compounds were between -4.00 ± 0.00 and -5.03 ± 0.38 Kcal/mol (*Supplementary table 3 and Figure 15*). The control drug that obtained the strongest binding energy (-7.50 ± 0.08 Kcal/mol) was dolutegravir (DTG) and interacted with residues His12 and Lys101 by forming pi-cation interactions and interacted with Mg^{2+} present within the active site, furthermore by Van der Waals interactions it interacted with residues Asp9, Thr11, Glu37, Gly63, Ser64, Asn65, Glu97, Asn100 and Lys104. The most favorable binding energy (-5.03 ± 0.38 Kcal/mol) was with TDC-2M through the formation of a hydrogen bond with Asn100 and a bond between the carboxyl group of the compound and one of the Mg^{2+} ions present in the active site. Similarly, an unfavorable interaction between the amino group of the compound and Mg^{2+} was also present. In addition, attractive charge, salt bridge, alkyl and Van der Waals type interactions with residues Asp9, Asp61, Gln93, Gly94, Glu97, Ile96 and Lys101 (*Figure 16E*).

The binding energies found between the capsid protein (p24) and the compounds were between -5.00 ± 0.00 and -5.60 ± 0.00 Kcal/mol (*Supplementary table 3 and Figure 15*). The compound that presented the most favorable binding energy (-5.60 ± 0.00 Kcal/mol) was TODC-3M and interacted with residues Asn53, Leu56, Asn57, Gln63, Met66, Gln67, Leu69, Lys70, Ile73, Thr107 and Tyr130 (*Figure 16F*).

Finally, the interaction scores between the matrix protein (p17) of HIV-1 and the compounds ranged from -4.70 ± 0.00 to -5.37 ± 0.05 Kcal/mol (*Supplementary table 3 and Figure 15*). The most favorable binding energy (-5.37 ± 0.05 Kcal/mol) was with TDC-2M through forming of a hydrogen bond with Tyr81, an unfavorable interaction was obtained with Hys33 and Van der Waals interactions with Leu21, Arg22, Lys27, Tyr29, His33, Trp36, Ser77, Asn80, and Thr97 (*Figure 16G*).

The anti-HIV-1 effect of these compounds could be explained by the action on reverse transcriptase and/or viral protease, considering that the binding energies were more favorable when the compounds interacted with these proteins. Moreover, the possible mechanism of action of TODC-3M may be due to interaction with gp120.

Reverse transcriptase (RT) is a heterodimer enzyme (p66/p51) that converts viral single-stranded RNA into double-stranded proviral DNA [85]. There are two classes of drugs approved by the FDA. Nucleoside RT inhibitors (NRTI) have a similar structure to the natural substrate (dNTP) but lack the OH group in the 3' position and terminate chain synthesis, among these are AZT and ABC. The second group is non-nucleoside RT inhibitors (NNRTI) which bind to an allosteric site, changing the conformation of the enzyme, as is the case with EFV [86]. The latter show interactions with residues Leu100, Lys101, Lys103, Val106, Trp107, Val108, Val179, Tyr181, Tyr188, Val189, Gly190, Phe227, and Tyr318 of the p66 subunit and Glu138 of the p51 subunit [45, 46].

When the complexes between the compounds with RT were studied, it was observed that they all interacted with a large amount of the residues present in the NNRTI binding site. Interestingly, TODB-2M presented binding energy of -6.4 ± 0.0 Kcal/mol with RT; this interaction was through the formation of a hydrogen bond with Tyr318 and the carboxyl group of the compound. Similarly, alkyl-type bonds were present with Br and the residues of Pro95, Leu100, Val179, Tyr181, and Trp229. A Pi-sigma type bond was formed between Leu100 and the phenolic ring. Finally, hydrophobic van der Waals-type interactions with Lys101, Lys103, Val106, Phe227, Leu234, His235, Pro236, Pro238, Pro238, and Pro239 were observed (*Figure 17A*). The affinity for RT increased when the halogen Br was replaced by Cl, thus the TODC-2M compound had binding energy of -6.73 ± 0.09 Kcal/mol. Like TODB-2M, this compound formed a hydrogen bond with Tyr318 (3.21 \AA), but this time it did so by interacting with the oxygen found in the ortho position of the phenolic ring. Through its amino group, this compound interacted with Tyr188 and Trp229 forming pi-cation and pi-sigma covalent bonds, a pi-anion bond was also formed between the

carboxyl group of the compound and Tyr181. Finally, Van der Waals interactions were observed with the residues of Lys101, Lys102, Tyr183, Phe227, and His235 and alkyl interactions with Leu100, Lys103, Val106, and Leu234 (*Figure 17B*). TODC-3M presented binding energy of -6.1 ± 0.0 Kcal/mol with RT; this interaction occurred through the formation of Van der Waals-type interactions with Pro95, Lys104, Val179 and Gly190, in addition alkyl-type bonds were formed with the residues of Leu100, Val106, Tyr181, Tyr188, Phe227, Trp229 and Leu234. A Pi-Pi type bond was formed between Tyr181 and the phenolic ring. Finally, the formation of a salt bridge was observed between the carboxyl group of the compound and the Lys101 residue (*Figure 17C*). Tyramine YDC-3M had binding energy with RT of -6.5 ± 0.0 Kcal/mol. This compound did not form hydrogen bonds with any protein residue, but a non-covalent Pi-Pi type interaction between the phenyl ring and Tyr181 was present. Cl formed alkyl bonds with Pro95, Tyr181, Tyr188, Phe227, Trp229, and Leu234. The amino group formed carbon-hydrogen bonds with residues Lys101, His235, and Pro236; Van der Waals bonds were also present with Lys103, Val106, and Tyr318 (*Figure 17D*).

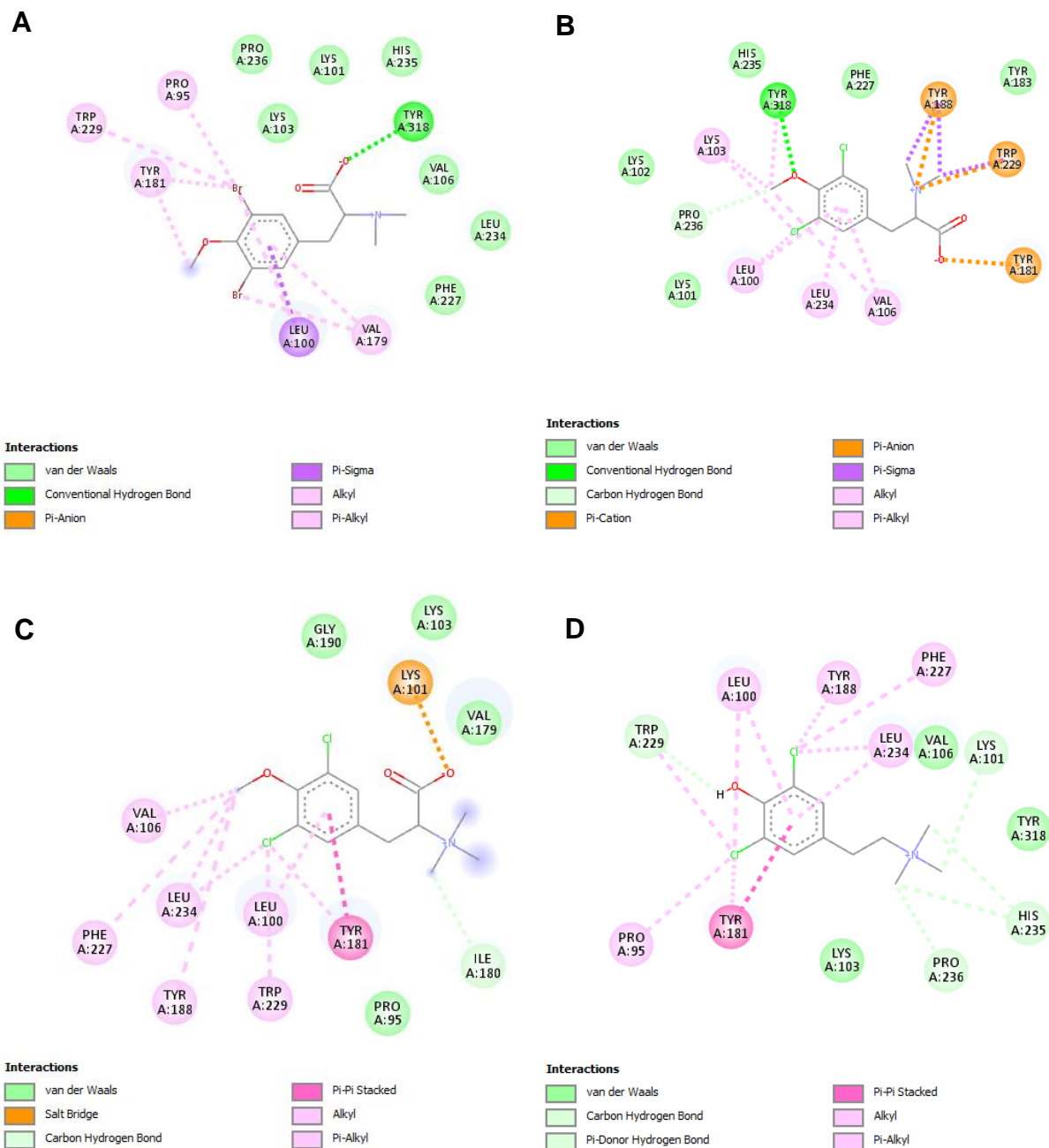


Figure 17. Interactions of TODB-2M, TODC-2M, TODC-3M and YDC-3M compounds with HIV-1 reverse transcriptase. A) TODB-2M. B) TODC-2M. C) TODC-3M. D) YDC-3M. Figures obtained by Discovery Studio show the possible site of the binding of the compounds with the viral reverse transcriptase.

HIV protease is a key enzyme in the viral replication process, as it is responsible for the maturation of the viral particles. It is an aspartyl protease consisting of two monomers of 99 amino acids. The aspartyl protease motif (catalytic triad: Asp25-Thr26-Gly27) is a key target for drug development

[87, 88]. There are currently multiple FDA-approved inhibitors of this enzyme, including ritonavir and lopinavir, which are catalytic active site competitive inhibitors [89, 90]. It was observed that our compounds interact directly with the key amino acids in the active site.

The TODB-2M compound, upon interaction with PR, had binding energy of -9.07 ± 0.5 Kcal/mol. It is a molecule that interacts, forming a hydrogen bond with the oxygen in the ortho position of the phenolic ring and Asp29'. It also forms salt bonds between Asp25 and Asp25' and the amino group. This phenolic ring also interacts with Asp25' forming a pi-anion bond. It forms carbon-hydrogen bonds with Ala28' and Gly48'. The halogen Br forms alkyl-type bonds with Val32', Ile47' and Ile84'. It also has Van der Waals interactions with Arg8, Gly27, Gly27', Ala28', Asp30', Gly49, Gly49', Ile50, Pro81' and Ile84. In addition, this compound exhibited an unfavorable negative-negative interaction between the carboxyl group and Asp25' (*Figure 18A*). TODC-2M upon interaction with PR had binding energy of -9.3 ± 0.0 Kcal/mol. It is a molecule that interacts forming a hydrogen bond with the oxygen at the ortho position of the phenyl ring and Asp29' and with the carboxyl group and Ile50. It also forms salt and carbon-hydrogen bonds between Asp25 and Asp25' and the amino group. It forms alkyl-type bonds with Ala28', Ile47' and Ile50. It also has Van der Waals interactions with Arg8, Gly27, Gly27', Ala28, Asp30', Val32', Gly48, Gly49, Gly49', Ile50', Pro81' and Ile84. In addition, this compound also showed an unfavorable negative-negative interaction between the carboxyl group and the Asp25' (*Figure 18B*). TODC-3M obtained the highest binding energy with PR being -9.37 ± 0.09 Kcal/mol; this interaction was produced by forming two hydrogen bonds and multiple Van der Waals interactions with other residues close to the active site, as previously described (*Figure 16D*). Finally, compound YDC-3M had binding energy with PR of -8.5 ± 0.0 Kcal/mol. This compound interacts forming two hydrogen bonds with Asp30, it also forms salt bonds between Asp25 and Asp25' and the amino group and carbon-hydrogen bonds with Ile50. It forms alkyl bonds between Val32 and Ile47' and the halogen Cl and between Ile50 and the phenolic ring. It also forms a Pi-sigma bond between Ala28 and the phenolic ring. It also has Van der Waals interactions with Gly27, Asp29, Gly49, Gly49', Leu76, Ile84, and Ile84' (*Figure 18C*).

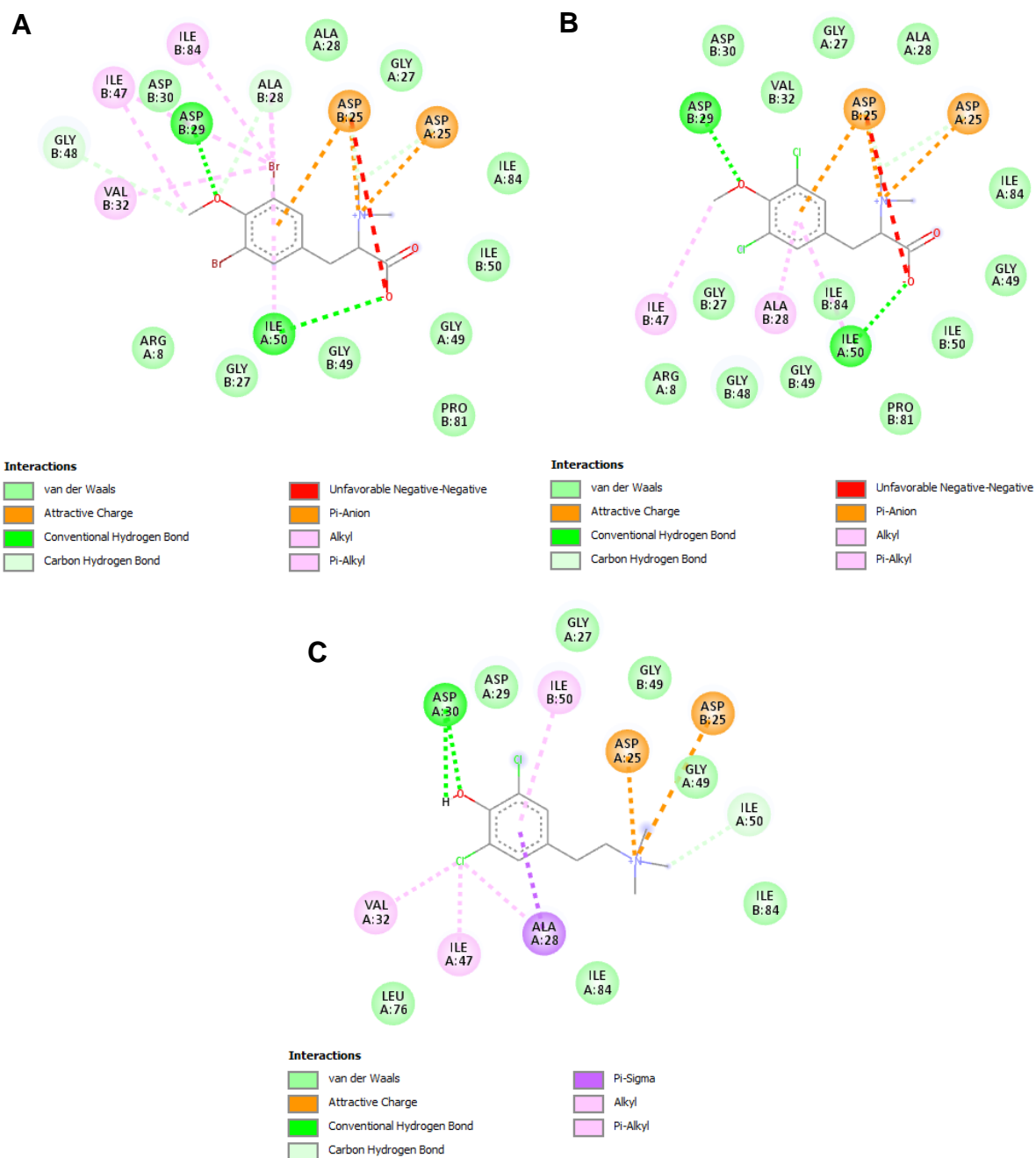


Figure 18. Interactions of TODB-2M, TODC-2M and YDC-3M compounds with HIV-1 protease. A) TODB-2M. B) TODC-3M. C) YDC-3M. Figures obtained by Discovery Studio show the possible site of the binding of the compounds with the viral protease.

Gp120 is a viral surface protein responsible for virus entry. It has five variable (V1-V5) and five constant (C1-C5) domains. The V3 loop is important for membrane fusion and co-receptor specificity, that is, the use of CCR5 versus CXCR4 [91]. TODC-3M value ($\Delta G_{\text{bind}} = -4.83 \pm 0.24$ Kcal/mol) forming Van der Waals interactions with the Trp112 residues, Val255, Ser256, Thr257,

Ile371, Ser375, Phe376, Phe382, Ile424, Asn425, Met426, Trp427, Gly473 and Met475. In addition, this compound presented an unfavorable negative-negative interaction between the carboxyl group and Asp368 and Glu370. (Figure 19).

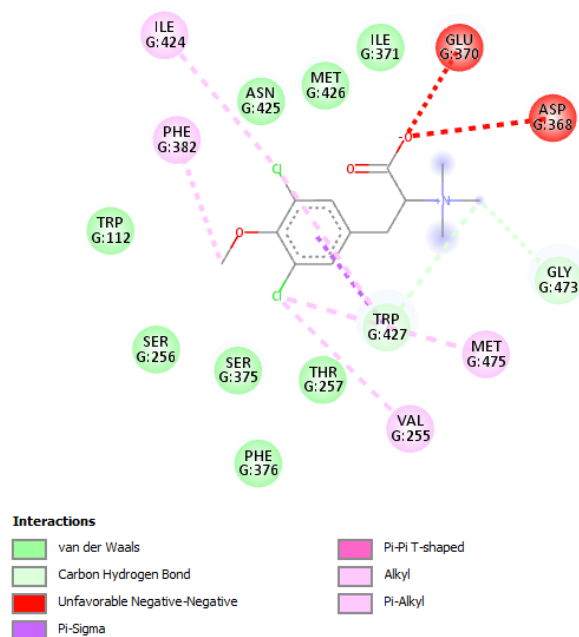


Figure 19. Interactions of TODC-3M compound with HIV-1 gp120. Figure obtained by Discovery Studio shows the possible site of the binding of the compounds with the viral gp120.

DISCUSSION

HIV/AIDS continues to be a public health problem worldwide. Despite the existence of combined treatment that reduces the circulating viral load to undetectable levels, there are problems of toxicity and resistance to the currently used drugs [92]; therefore, the search for new antiviral strategies continues.

In this study, we evaluated 16 synthetic di-halogenated compounds derived from L-tyrosine, which are structural derivatives of compounds previously isolated from the marine sponges *Verongula rigida* and *Aiolochoia crassa* [60].

The discovery and development of a new drug is a costly and time-consuming process; therefore, in recent years, ADMET technology has been adopted to predict the pharmacological potential of a compound and thus avoid failure [93]. The compounds presented in our study have low and

medium cumulative toxicity, like the control drugs evaluated (*Table 4*). Only the compounds in YODB-2M, YODB-3M, YODC-2, and YODC-3M were predicted to be toxic because they had a neurotoxic effect by inducing phospholipids and a cardiac effect by blocking hERG channels. In the ADMET_Risk variable, which serves as a comprehensive filter that includes 24 parameters addressing absorption, metabolism, toxicity, and pharmacokinetic parameters associated with the five rules of Lipinski [94], all our compounds obtained a minimal overall risk as they had a score below 7, and they were even improved in some respect than the control drugs lopinavir and ritonavir with scores of 7.5 and 9.7, respectively (*Table 4*). Therefore, di-halogenated compounds with potent antiviral activity (*Supplementary table 1 and 2*) would be appropriate candidates as oral drugs.

In our study, the *in vitro* cytotoxicity of these compounds was initially evaluated in TZM-bl cells. Cell viability higher than 77% at a concentration of 150 μM for all compounds except YDB-3M was found (*Figure 2*). These data are congruent with those reported for other halogenated L-tyrosines, where *in vitro* cytotoxicity lower than 25% was reported in the U373-MAGI cell line treated with concentrations ≤ 320 μM [60]. Similarly, our collaborators found cell viability of VERO cells up to 90% when treated with L-tyrosine-derivates compounds with free phenolic OH at a concentration of 250 μM [95]. With these results, we calculated the CC_{50} for each compound, where we ruled out a cytotoxic effect as a potential mechanism to explain the viral inhibition.

According to the *in silico* and *in vitro* cytotoxicity results, the compounds showed low toxicity and could be evaluated at subsequent stages; however, studies in other non-tumor cell and *in vivo* models are needed to know the safety profile of the compounds.

Other compounds derived from L-tyrosine structurally related to ours have been previously reported for their antiviral activity against HIV-1 [60, 96, 97], respiratory syncytial virus, [98] and SARS-CoV-2 [99, 100]. In contrast, in our study, the compounds presented the variable activity to inhibit the HIV-1 infection, depending on the strain evaluated and the structural modifications of each compound.

We included a combined antiviral screening strategy to evaluate the antiviral effect of the 16 compounds in HIV-1 infection. The HIV-1 BaL (R5) strain was used as a viral model since this virus is predominantly detected during early infection. In the natural course of infection, individuals become infected with this strain, but in the more chronic stages of infection, a change of tropism occurs [101]. The tropism shift from R5 to X4 strain is associated with accelerated CD4^+

T cell depletion and disease progression and is primarily explained by modifications in the region of gp120 that encodes the V3 loop [102]. The HIV-1_{IIIB} (X4) strain was used to evaluate this model. In addition, HIV-GFP-VSV-G, which does not have the HIV envelope, but instead uses the vesicular stomatitis virus envelope for entry; was used as a model to evaluate the inhibition of the replicative cycle after entry. Thus, the differences in antiviral activity between the R5 and X4 strains suggest different times in the development of virus infection. This, coupled with the HIV-GFP-VSV-G pseudotyped virus assays will allow us to determine whether the compounds act by inhibiting early or late stages of infection, and thus determine the possible mechanism of action involved in the antiviral activity.

The brominated compounds TDB-2M and TDB-3M did not inhibit the replicative activity of the strains tested. In contrast, the chlorinated compounds TDC-2M and TDC-3M showed antiviral activity in the R5 strain, while no antiviral activity in the X4 strain was observed (*Supplementary table 1 and 2*). These compounds were also evaluated by colleagues against other viral models; it was observed that all of them increased the production of infectious dengue virus -2 particles, but showed a potential to significantly inhibited the production of infectious viral particles of chikungunya virus, with inhibition percentages between 60,1% and 71,5% [95]. That suggests, that the antiviral activity of these compounds depends on the viral model evaluated, and that the inhibition of HIV replicative activity is not affected by exposure to brominated L-tyrosine-derivates with free phenolic OH compounds, probably due to a factor inherent to the viral infection.

For methyl ether L-tyrosine-derivates compounds, TODB-2M inhibited strains R5 and X4, while its respective quaternary ammonium salt (TODB-3M) showed no activity against any of the strains tested. TODC-2M inhibited replication of strain R5 and strain X4. In addition, TODC-3M effectively inhibited replication of strain R5 (*Supplementary table 1 and 2*). To date, there are no other studies evaluating the antiviral activity of these methyl ether L-tyrosine-derivates compounds in this viral model or in others, but several authors have evaluated the activity of bromotyrosines derived from marine sponges such as mololipids [103], psammalyssine D [104], aeropylsinin-1 [60], fistularin-3 [105], purealidin B [60] and observed antiviral activity against different HIV-1 strains evaluated (e.g Haitian RF strain of HIV-1, HIV-GFP-VSV-G virus), attributing their activity to the inhibition of different steps of the HIV replicative cycle. This can be extrapolated with this study due to the structural similarity with our compounds, since all of them are tyrosine derivatives and present di-halogenation with Br in the structure.

The structural difference between TDB-2M and TODB-2M is the addition of a methyl group on the free phenolic OH. Interestingly, this structural difference appears to favor the antiviral activity of the compound, such as was observed for TDC-3M and TODC-3M. This opens the door to new studies in which modifications such as the addition of methyl groups in compounds with antiviral potential could enhance their activity as potential therapeutic agents against HIV.

In tyramine-derivates compounds, YDB-2M had no antiviral activity against strains R5 or X4. The quaternary ammonium salt YDB-3M inhibited replication of strain X4 at the lowest concentration tested but had no activity against strain R5. At the highest concentration evaluated the compounds YDB-2M and YDB-3M may produce an increase in strains R5 HIV-1 replication (*Supplementary table 1 and 2*). This effect may be due to the action of the compound on TZM-bl cells, increasing cell proliferation, enhancing cell metabolism or gene transcription and consequently increasing cellular and viral proteins synthesis. Our collaborators observed a similar effect in the Zika viral model, with di-halogenated compounds with chlorine and bromine structurally similar to ours [95]. However, further studies are needed to elucidate how viral replication is enhanced. The chlorinated analogue YDC-2M also had no activity against the strains tested, while YDC-3M inhibited replication of both strains. Unexpectedly, an inverse relationship was observed between YDC-3M concentration and the anti-HIV-1 activity. This means that the inhibitory activity decreases as the YDC-3M concentration increases. Higher concentrations of the compound are not optimal for achieving its antiviral activity. At these concentrations the compounds may produce saturation of TZM-bl cells, preventing the entry of the compound or the interaction with viral proteins, which may be detrimental to the evaluation of the antiviral effect. Finally, methyl ether tyramine-derivates compounds were the least active against the virus, as only YODB-3M had anti-HIV activity, inhibiting the replication of strain X4. At 75 μ M, the compound YODB-2M increased the replication of HIV-1 strains R5 and X4 (*Supplementary table 1 and 2*). As with the brominated analogues of tyramine-derivates with free phenolic OH compounds, this effect may be due to the action of the compounds on the cells, increasing cell proliferation, enhancing cell metabolism or gene transcription and consequently increasing cellular and viral proteins synthesis. Other compounds derived from bromotyrosines have exhibited variable ability to inhibit HIV-1 replication *in vitro*, among these are YDB-3M and YODB-3M. The latter inhibited HIV-1 entry (X4 strain) in a dose-dependent manner, but neither compound had activity against the R5 strain [60]. These results are congruent with those found by us.

Following the antiviral screening, four compounds with the highest inhibitory capacity against viral strains were selected and evaluated against a pseudotyped virus (HIV-GFP-VSV-G). TODB-2M, TODC-2M, and YDC-3M compounds obtained an inhibition percentage between 12.5 - 44.2% (Figure 14). Likewise, these compounds had an antiviral effect when evaluated with R5 and X4 strains; this suggests that the mechanism of action of these compounds may be due to interactions with viral proteins involved in the replication steps that occur after virus entry. This mechanism, coupled with *in silico* assays, may indicate that inhibition of viral replication is due to interaction with protease or RT. The TODC-3M compound did not exhibit antiviral activity using HIV-GFP-VSV-G, as with the X4 strain. This suggests that the possible mechanism of action is at virus entry, by interacting with gp120 of the R5 strain. Wu ZY *et al.*, observed that di-brominated compounds, such as diarylpyridinamine analogues (DAPA), favored antiviral activity over di-chlorinated compounds against wild-type HIV-1 NL4-3 (X4 strain) infection in TZM-bl cells. [106]. These results are consistent with ours when using the X4 strain, where it was observed that three of the five compounds exhibiting antiviral activity were di-brominated. In contrast, higher antiviral activity was observed when the di-chlorinated compounds were used against the R5 strain.

Interestingly, by using HIV-GFP-VSV-G as a viral model, the TODB-2M compound showed the highest percentage of inhibition; this compound has two Br halogens in its structure, while the activity of di-chlorinated compounds was significantly lower. Our study suggests that these compounds could be promisor to evaluate in studies as potential anti-HIV-1 drugs.

Although the concentrations at which the di-halogenated compounds had an antiviral effect are higher than the AZT concentration, it is important to consider that this drug is potentially toxic [107]. In addition, although the compound concentrations with antiviral activity were not toxic in the cells evaluated, it is important to carry out *in vivo* studies to determine whether these concentrations are safe. Therefore, searching for new molecules with a safer pharmacological profile is necessary.

Molecular docking is a frequently used methodology for designing and discovering new bioactive molecules due to the potential to simulate interactions between a ligand and a target and predict the binding mode and affinity between them, thus predicting whether it can produce the expected biological effect [108, 109]. In our study, all 16 compounds interacted with viral RT and PR. In addition, compounds YDC-2M and YODC-2M complied with the threshold when interacting with gp120 (Supplementary table 3 and Figure 15). In this case, we observed a higher affinity score for

compounds with Cl in their structure, which is congruent with that found by *Bollini et al.*, who observed that chlorine substitution in the terminal phenolic ring predicts more favorable binding energies with RT [110]. The anti-HIV-1 effect of TODB-2M, TODC-2M and YDC-3M compounds could be attributed to action on viral RT and/or PR, since the binding energies were more favorable upon interaction with these proteins. The TODC-3M compound in addition to interacting with these proteins, action may be due to inhibition of entry by interacting with gp120.

RT is an enzyme that converts viral single-stranded RNA into double-stranded proviral DNA [111]. The results presented in this work agree with those obtained by *Ortega et al.* when evaluating the antiviral activity of myricetin derivatives as NNRTIs against HIV-1_{IIIIB} (strain X4), because the binding interactions of our compounds also occurred with residues of the hydrophobic NNRTI-binding pocket (*Figure 17*), specifically with residues Leu100, Lys101, Lys103, Val106, Val179, Tyr181, Tyr188, Phe227, Trp229, and Tyr318 of p66 subunit [112]. Likewise, it has been described that nevirapine (FDA-approved drug as an NNRTI) acts against RT by binding to this hydrophobic pocket specifically [113, 114]. Therefore, our compounds TODB-2M, TODC-2M and YDC-3M could be working as NNRTIs.

HIV protease is responsible for the maturation of the viral particles. The protease active site is formed by the catalytic triad: Asp25-Thr26-Gly27, this region is a crucial target for drug development [87, 88]. Our study observed that TODB-2M, TODC-2M and YDC-3M compounds interact directly with the critical amino acids in the active site (*Figure 18*); these interactions could enhance the inhibitory effect by blocking the structure in its closed conformation and thus hindering the entry of natural substrates.

Gp120 is the viral protein that mediates entry into the host cell by interacting with the CD4 receptor and a coreceptor (CCR5 or CXCR4) [115]. The drug fostemsavir binds to this protein and interacts with residues Asp425, Met426 and Trp427 and alters their conformation, blocking subsequent binding to the CD4 receptor [116]. Our study predicted that the compound TODC-3M interacted with these crucial residues in the protein binding to the receptor (*Figure 19*), indicating a similar effect to fostemsavir, blocking entry.

In our study, 16 compounds were evaluated and modified with bromine and chlorine halogens. The use of halogenated compounds can give an advantage for the design of new drugs due to the formation of halogen bonds (X) formed by chlorine (Cl), bromine (Br), and iodine (I), which are comparable to hydrogen bonds and can increase the protein-ligand affinity [117, 118]. Previous

studies have shown that the presence of Br in the molecules improves the selectivity of protein-ligand interactions, while the presence of Cl improves the pharmacokinetic properties [119]. The results obtained in this study open the door to further investigations of di-halogenated compounds as potential lead compounds; that is, molecules or chemical compounds that can be optimized from the initial molecule to improve the activity, potency and selectivity of the compound to progress towards the development of antiviral agents.

CONCLUSION

TODB-2M, TODC-2M, TODC-3M and YDC-3M are new synthetic di-halogenated compounds derived from L-tyrosine that could be considered as lead compounds to develop a promising anti-HIV-1 agent. According to biological activity assays, TODB-2M, TODC-2M and YDC-3M compounds showed inhibitory activity against HIV-1 replication viruses with CCR5 and CXCR4 tropism and a pseudotyped virus, while TODC-3M was effective against CCR5 tropic virus. These compounds demonstrated antiviral activity, but the mechanism of action has not yet been elucidated experimentally; however, based on the viral models used in our study, we can hypothesize that TODB-2M, TODC-2M and YDC-3M act by inhibiting steps downstream of viral entry; while TODC-3M would inhibit steps upstream of entry. According to *in silico* results, the possible mechanism is the interaction with reverse transcriptase and/or viral protease, or with the envelope protein in the case of TODC-3M. In addition, the *in vitro* and *in silico* methodology used in this study are valuable tools for studying antivirals, determining possible mechanisms of action and toxic effects associated with the chemical nature of different compounds.

LIMITATIONS AND PERSPECTIVES OF THE STUDY

In vitro evaluation of the antiviral activity using the pre-infection and post-infection treatment screening strategy within the same experimental unit, allows elucidating the antiviral activity of the compounds on R5 and X4 strains, but not the step of the replicative cycle that they inhibit. For this reason, in addition to these viral models, we used a pseudotyped virus that allowed us to evaluate the antiviral activity of the compounds in the post-entry steps, but the exact mechanism of action has not yet been elucidated. Therefore, it is necessary to evaluate by other strategies different steps of the HIV replicative cycle to confirm the hypotheses proposed.

Similarly, the present study was performed in transformed human cells (TZM-bl). Evaluation in target cells of the infection such as peripheral blood mononuclear cells (PBMC), may provide closer information on a possible antiviral response, so it can be considered as a perspective to be evaluated.

Furthermore, it is important to evaluate the toxicity of these promising compounds *in vivo* models to determine the systemic toxicity that is not possible to achieve through cellular assays and thus correlate *in vivo* results with those found *in vitro* and *in silico*.

The *in silico* methodology evaluated the binding energies with wild-type viral proteins; in this context, performing *in silico* assays with drug-resistant proteins would be helpful. In addition, only the interactions of the compounds with gp120 of the R5 strain were evaluated; we intend to perform molecular docking with the X4 strain. Likewise, molecular dynamics studies between protease, reverse transcriptase and gp120 will allow us to know the stability of these proteins in complex with the most promising compounds and thus support or reject the hypotheses proposed.

ADDITIONAL INFORMATION

The results of this study were presented at the following events:

- “Primer encuentro de Modelamiento Molecular Colombia (MMCol)” 2020.
- “IX Simposio Colombiano de Virología y V Congreso Latinoamericano de Virología” 2021.
- “XIII Encuentro Nacional de Investigación en Enfermedades Infecciosas y III Encuentro Latinoamericano de Investigación en Enfermedades Infecciosas” 2022.





La Institución Universitaria Visión de las Américas y la Asociación Colombiana de Virología

Certifica que:


Maria S. Serna-Arbelaez^{1,2}, Vanessa Loaiza-Cano², Marlen Martinez-Gutierrez², Elkin Galeano⁴, Wildeman Zapata^{1,3}


Participaron con el trabajo:

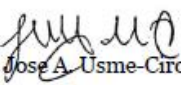
Actividad antiviral in vitro e in silico de compuestos di-halogenados derivados de L-tirosina contra el virus de la Inmunodeficiencia Humana 1 (VIH-1)

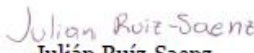
En la modalidad Presentación Oral durante el:

“IX Simposio Colombiano de Virología y V Congreso Latinoamericano de Virología” realizado los días 17 a 19 de Noviembre de 2021


Jaime A. Cardona-Ospina
Presidente
Comité Organizador


Alfonso J. Rodríguez-Morales
Presidente Honorario
Comité Organizador


Jose A. Usme-Ciro
Presidente
Junta Directiva


Julián Ruiz-Saenz
Presidente
Comité Científico

XIII

*Encuentro Nacional de Investigación en
Enfermedades Infecciosas*

*III Encuentro Latinoamericano de
Investigación en Enfermedades Infecciosas*

18 a 20 de agosto de 2022 Hotel Spiwak / Cali



La Asociación Colombiana de Infectología - ACIN

Certifica que:

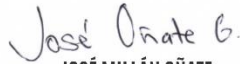
MARÍA SULENY SERNA ARBELÁEZ

Participó en calidad de ponente,

En el marco del XIII Encuentro Nacional de Investigación en Enfermedades Infecciosas
y III Encuentro Latinoamericano de Investigación en Enfermedades Infecciosas

Realizado los días 18 al 20 de agosto de 2022

Intensidad horaria 24 horas



José Oñate O.

JOSÉ MILLÁN OÑATE

Presidente XIII Encuentro Nacional de
Investigación en Enfermedades Infecciosas



ALFONSO J. RODRÍGUEZ MORALES

Presidente Asociación
Colombiana de Infectología - ACIN



REFERENCES

1. (CDC), C.f.D.C., *Pneumocystis pneumonia--Los Angeles*. MMWR. Morbidity and mortality weekly report, 1981. **30**(21).
2. UNAIDS. *Global HIV & AIDS statistics — Fact sheet*. 2022 [cited 2022 July 9]; Available from: <https://www.unaids.org/en/resources/fact-sheet>.
3. Costo, C.d.A. *Situación del VIH y sida en Colombia 2021 | Cuenta de Alto Costo*. 2021 [cited 2022 July 9]; Available from: <https://cuentadealtocosto.org/site/publicaciones/situacion-del-vih-y-sida-en-colombia-2021/>.
4. A, A., et al., *HIV Antiretroviral Medication Neuropenetrance and Neurocognitive Outcomes in HIV+ Adults: A Review of the Literature Examining the Central Nervous System Penetration Effectiveness Score*. *Viruses*, 2022. **14**(6).
5. *Understanding Fast-Track: accelerating action to end the AIDS epidemic by 2030*. 2015; Available from: <https://digitallibrary.un.org/record/3948651>.
6. Y, H., T. L, and U. T, *Prescribing for patients taking antiretroviral therapy*. *Australian prescriber*, 2022. **45**(3).
7. Melhuish, A.L., Penny., *Natural history of HIV and AIDS*. *Medicine*, 2022. **50**(5).
8. V, S., H. DD, and A.K. Q, *HIV/AIDS epidemiology, pathogenesis, prevention, and treatment*. *Lancet (London, England)*, 2006. **368**(9534).
9. AD, L., *Genetic barriers to resistance and impact on clinical response*. *MedGenMed : Medscape general medicine*, 2005. **7**(3).
10. PS, P., *HIV Drug Resistance: Problems and Perspectives*. *Infectious disease reports*, 2013. **5**(Suppl 1).
11. SA, I., I. DG, and J. G, *Improving the Adherence to Antiretroviral Therapy, a Difficult but Essential Task for a Successful HIV Treatment-Clinical Points of View and Practical Considerations*. *Frontiers in pharmacology*, 2017. **8**.
12. Montessori V, P.N., Harris M, Akagi L, Montaner JS., *Adverse effects of antiretroviral therapy for HIV infection*. *CMAJ*, 2004. **170**(2): p. 229-238.
13. SG, D., L. SR, and H. DV, *The end of AIDS: HIV infection as a chronic disease*. *Lancet (London, England)*, 2013. **382**(9903).
14. CP, P. and S.-C. A, *HIV cure research: advances and prospects*. *Virology*, 2014. **454-455**.
15. ICTV. *National Institutes of Health. International committee on Taxonomy of virus*. 2022 [cited 2022 July 9]; Available from: https://talk.ictvonline.org/ictv-reports/ictv_online_report/reverse-transcribing-dna-and-rna-viruses/w/retroviridae/1704/genus-lentivirus.
16. BS, T., et al., *The challenge of HIV-1 subtype diversity*. *The New England journal of medicine*, 2008. **358**(15).
17. J, E. and G. L, *HIV types, groups, subtypes and recombinant forms: errors in replication, selection pressure and quasispecies*. *Intervirology*, 2012. **55**(2).
18. GM, S. and H. E, *HIV transmission*. *Cold Spring Harbor perspectives in medicine*, 2012. **2**(11).
19. K, K., T. NH, and A. GM, *HIV and SIV in Body Fluids: From Breast Milk to the Genitourinary Tract*. *Current immunology reviews*, 2019. **15**(1).
20. KK, V.V., et al., *Pathophysiology of CD4+ T-Cell Depletion in HIV-1 and HIV-2 Infections*. *Frontiers in immunology*, 2017. **8**.
21. AA, L., L. MM, and R. B, *HIV pathogenesis: the host*. *Cold Spring Harbor perspectives in medicine*, 2012. **2**(9).

22. CB, W., T. JC, and D. RW, *HIV: cell binding and entry*. Cold Spring Harbor perspectives in medicine, 2012. **2**(8).
23. MR, F., et al., *HIV-1 replication cycle*. Clinics in laboratory medicine, 2002. **22**(3).
24. ME, G., *The HIV-1 Vpr Protein: A Multifaceted Target for Therapeutic Intervention*. International journal of molecular sciences, 2017. **18**(1).
25. AK, S. and D. K, *Insights into HIV-1 Reverse Transcriptase (RT) Inhibition and Drug Resistance from Thirty Years of Structural Studies*. Viruses, 2022. **14**(5).
26. YH, S., P. CM, and Y. CH, *An Overview of Human Immunodeficiency Virus-1 Antiretroviral Drugs: General Principles and Current Status*. Infection & chemotherapy, 2021. **53**(1).
27. FE, Y., *The role of the FDA in the effort against AIDS*. Public health reports (Washington, D.C. : 1974), 1988. **103**(3).
28. FDA, *The History of FDA's Role in Preventing the Spread of HIV/AIDS | FDA*. 2019, @US_FDA.
29. AA, H. and T. JC, *Entry inhibitors and their use in the treatment of HIV-1 infection*. Antiviral research, 2013. **98**(2).
30. MA, C., L. BG, and F. EO, *HIV-1 envelope glycoprotein biosynthesis, trafficking, and incorporation*. Journal of molecular biology, 2011. **410**(4).
31. C, T., et al., *Viral surface glycoproteins, gp120 and gp41, as potential drug targets against HIV-1: brief overview one quarter of a century past the approval of zidovudine, the first anti-retroviral drug*. European journal of medicinal chemistry, 2011. **46**(4).
32. NA, M., et al., *Inhibitors of HIV-1 Attachment: The Discovery and Development of Temsavir and its Prodrug Fostemsavir*. Journal of medicinal chemistry, 2018. **61**(1).
33. C, M., et al., *Efficacy and Safety Profile of Fostemsavir for the Treatment of People with Human Immunodeficiency Virus-1 (HIV-1): Current Evidence and Place in Therapy*. Drug design, development and therapy, 2022. **16**.
34. SJ, A., et al., *Comparative Efficacy and Safety of Fostemsavir in Heavily Treatment-Experienced People With HIV-1*. Clinical therapeutics, 2022. **44**(6).
35. N, S., F. C, and K. M, *Fostemsavir for the treatment of HIV*. Expert review of anti-infective therapy, 2021. **19**(8).
36. SM, W. and K. GD, *Maraviroc: a review of its use in HIV infection and beyond*. Drug design, development and therapy, 2015. **9**.
37. CM, P., *Maraviroc: a review of its use in the management of CCR5-tropic HIV-1 infection*. Drugs, 2010. **70**(9).
38. JC, W., R. JK, and H. WD, *Drug safety evaluation of maraviroc for the treatment of HIV infection*. Expert opinion on drug safety, 2012. **11**(1).
39. M, P., et al., *Structure and immune recognition of trimeric pre-fusion HIV-1 Env*. Nature, 2014. **514**(7523).
40. T, M., et al., *Enfuvirtide: the first therapy to inhibit the entry of HIV-1 into host CD4 lymphocytes*. Nature reviews. Drug discovery, 2004. **3**(3).
41. V, J., et al., *Enfuvirtide: from basic investigations to current clinical use*. Expert opinion on pharmacotherapy, 2010. **11**(16).
42. TM, D. and P. CM, *Enfuvirtide*. Drugs, 2003. **63**(24).
43. RL, S., et al., *Conformational Changes in HIV-1 Reverse Transcriptase that Facilitate Its Maturation*. Structure (London, England : 1993), 2019. **27**(10).
44. DM, H., et al., *Structure of HIV-1 reverse transcriptase with the inhibitor beta-Thujaplicinol bound at the RNase H active site*. Structure (London, England : 1993), 2009. **17**(12).

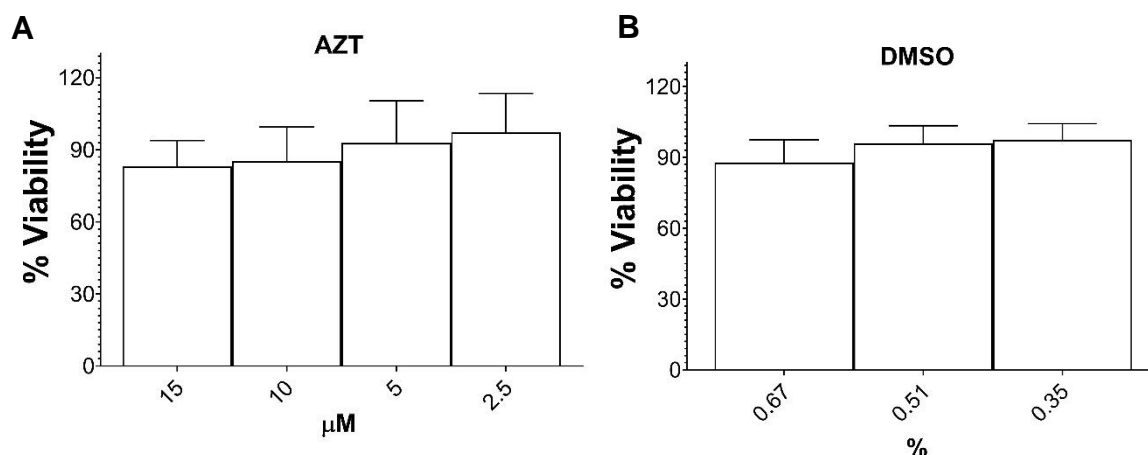
45. N, S.-C., T. NA, and B. I, *Conformational changes in HIV-1 reverse transcriptase induced by nonnucleoside reverse transcriptase inhibitor binding*. Current HIV research, 2004. **2**(4).
46. O, T., P. V, and V. A, *Molecular Docking Studies of HIV-1 Resistance to Reverse Transcriptase Inhibitors: Mini-Review*. Molecules (Basel, Switzerland), 2018. **23**(5).
47. E, D.C., *Anti-HIV drugs: 25 compounds approved within 25 years after the discovery of HIV*. International journal of antimicrobial agents, 2009. **33**(4).
48. PH, P. and Z. H, *Reverse Transcriptase Inhibitors*. 2022.
49. J, T., et al., *Recent Advances in the Development of Integrase Inhibitors for HIV Treatment*. Current HIV/AIDS reports, 2020. **17**(1).
50. ML, B., et al., *Induced-fit docking approach provides insight into the binding mode and mechanism of action of HIV-1 integrase inhibitors*. ChemMedChem, 2009. **4**(9).
51. A, K., et al., *Update on Adverse Effects of HIV Integrase Inhibitors*. Current treatment options in infectious diseases, 2019. **11**(4).
52. JM, L., et al., *HIV-1 protease: structure, dynamics, and inhibition*. Advances in pharmacology (San Diego, Calif.), 2007. **55**.
53. JG, K. and S. L, *Beyond Inhibition: A Novel Strategy of Targeting HIV-1 Protease to Eliminate Viral Reservoirs*. Viruses, 2022. **14**(6).
54. JB, C., *The role of natural products in modern drug discovery*. Anais da Academia Brasileira de Ciencias, 2019.
55. Nacheja, J.B., et al., *HIV treatment adherence, drug resistance, virologic failure: evolving concepts*. Infect Disord Drug Targets, 2011. **11**(2): p. 167-74.
56. Gardner, E.M., et al., *Antiretroviral medication adherence and the development of class-specific antiretroviral resistance*. AIDS, 2009. **23**(9): p. 1035-46.
57. WHO, *Fact Sheet: HIV Drug Resistance*. 2021, World Health Organization.
58. Bergmann, W. and R.J. Feeney, *Contributions to the study of marine products. xxxii. the nucleosides of sponges. i.1*. 2002.
59. H, M., et al., *3'-Azido-3'-deoxythymidine (BW A509U): an antiviral agent that inhibits the infectivity and cytopathic effect of human T-lymphotropic virus type III/lymphadenopathy-associated virus in vitro*. Proceedings of the National Academy of Sciences of the United States of America, 1985. **82**(20).
60. Rugeles, M.T., et al., *Bromotyrosine derivatives from marine sponges inhibit the HIV-1 replication in vitro*. Vitae, 2014. **21**(2): p. 114-125.
61. Pastrana Restrepo, M., et al., *Synthesis and trypanocide activity of chloro-l-tyrosine and bromo-l-tyrosine derivatives*. Medicinal Chemistry Research, 2018. **27**(11): p. 2454-2465.
62. M, M., et al., *Anti-HIV-1 activity, protease inhibition and safety profile of extracts prepared from Rhus parviflora*. BMC complementary and alternative medicine, 2013. **13**.
63. EJ, P., et al., *Effects of CCR5 and CD4 cell surface concentrations on infections by macrophagetropic isolates of human immunodeficiency virus type 1*. Journal of virology, 1998. **72**(4).
64. X, W., et al., *Emergence of resistant human immunodeficiency virus type 1 in patients receiving fusion inhibitor (T-20) monotherapy*. Antimicrobial agents and chemotherapy, 2002. **46**(6).
65. M, S.-K., et al., *Optimization and validation of the TZM-bl assay for standardized assessments of neutralizing antibodies against HIV-1*. Journal of immunological methods, 2014. **409**.
66. S, G., et al., *The role of mononuclear phagocytes in HTLV-III/LAV infection*. Science (New York, N.Y.), 1986. **233**(4760).

67. Y, L., et al., *CD4-independent infection of astrocytes by human immunodeficiency virus type 1: requirement for the human mannose receptor*. Journal of virology, 2004. **78**(8).
68. W, Z., et al., *Identification of innate immune antiretroviral factors during in vivo and in vitro exposure to HIV-1*. Microbes and infection, 2016. **18**(3).
69. S, P., P. V, and M. RM, *Anti-HIV-1 activity of flavonoid myricetin on HIV-1 infection in a dual-chamber in vitro model*. PloS one, 2014. **9**(12).
70. Avogadro, *Avogadro: an open-source molecular builder and visualization tool*. 2022, @AvogadroChem.
71. Hanwell, M.D., et al., *Avogadro: an advanced semantic chemical editor, visualization, and analysis platform*. Journal of Cheminformatics, 2012. **4**(1): p. 1-17.
72. GM, M., et al., *AutoDock4 and AutoDockTools4: Automated docking with selective receptor flexibility*. Journal of computational chemistry, 2009. **30**(16).
73. O, V., et al., *Active site binding modes of curcumin in HIV-1 protease and integrase*. Bioorganic & medicinal chemistry letters, 2005. **15**(14).
74. L, K. and E. A, *Retroviral integrase proteins and HIV-1 DNA integration*. The Journal of biological chemistry, 2012. **287**(49).
75. MF, S., *Python: a programming language for software integration and development*. Journal of molecular graphics & modelling, 1999. **17**(1).
76. A, L., et al., *Detection of peptide-binding sites on protein surfaces: the first step toward the modeling and targeting of peptide-mediated interactions*. Proteins, 2013. **81**(12).
77. R, B., et al., *Fragment-based identification of druggable 'hot spots' of proteins using Fourier domain correlation techniques*. Bioinformatics (Oxford, England), 2009. **25**(5).
78. O, T. and O. AJ, *AutoDock Vina: improving the speed and accuracy of docking with a new scoring function, efficient optimization, and multithreading*. Journal of computational chemistry, 2010. **31**(2).
79. S, S. and F. C, *In silico predictive model to determine vector-mediated transport properties for the blood-brain barrier choline transporter*. Advances and applications in bioinformatics and chemistry : AABC, 2014. **7**.
80. Sampangi-Ramaiah, M.H., Vishwakarma, Ram, Shaanker, R. Uma, *Molecular docking analysis of selected natural products from plants for inhibition of SARS-CoV-2 main protease*. 2020.
81. M, V., et al., *In silico identification of potential inhibitors against main protease of SARS-CoV-2 6LU7 from Andrographis paniculata via molecular docking, binding energy calculations and molecular dynamics simulation studies*. Saudi Journal of Biological Sciences, 2021. **29**(1): p. 18-29.
82. BIOVIA, *[Discovery Studio Visualizer v21.2.0.20298]*, D. Systèmes, Editor. 2021: San Diego: Dassault Systèmes.
83. www.simulations-plus.com. 2022; Available from: www.simulations-plus.com.
84. Maechler M, R.P., Struyf A, Hubert M, Hornik K, *Cluster Analysis Basics and Extensions*. 2022.
85. RE, L., *HIV-1 Reverse Transcriptase: A Metamorphic Protein with Three Stable States*. Structure (London, England : 1993), 2019. **27**(3).
86. SX, G., et al., *Recent discoveries in HIV-1 reverse transcriptase inhibitors*. Current opinion in pharmacology, 2020. **54**.
87. G, L.M., et al., *Off-Target-Based Design of Selective HIV-1 PROTEASE Inhibitors*. International journal of molecular sciences, 2021. **22**(11).
88. L, H. and C. C, *Understanding HIV-1 protease autoprocessing for novel therapeutic development*. Future medicinal chemistry, 2013. **5**(11).

89. Z, L., C. Y, and W. Y, *HIV protease inhibitors: a review of molecular selectivity and toxicity*. HIV/AIDS (Auckland, N.Z.), 2015. **7**.
90. Yoosefian, M.M., MZ. Juan, Alfredo, *In silico evaluation of atazanavir as a potential HIV main protease inhibitor and its comparison with new designed analogs*. Computers in Biology and Medicine, 2022. **145**(105523).
91. P, T. and F. CA, *Molecular recognition of CCR5 by an HIV-1 gp120 V3 loop*. PloS one, 2014. **9**(4).
92. TM, T., et al., *Insights Into Persistent HIV-1 Infection and Functional Cure: Novel Capabilities and Strategies*. Frontiers in microbiology, 2022. **13**.
93. H, v.d.W. and G. E, *ADMET in silico modelling: towards prediction paradise?* Nature reviews. Drug discovery, 2003. **2**(3).
94. Clark, R.D., et al., *Design and tests of prospective property predictions for novel antimalarial 2-aminopropylaminoquinolones*. Journal of Computer-Aided Molecular Design, 2020. **34**(11): p. 1117-1132.
95. Loaiza-Cano V, M.-E.L., Restrepo MP, and P.M.S. Quintero-Gil DC, Galeano E, Zapata W, Martinez-Gutierrez M, *In Vitro and In Silico Anti-Arboviral Activities of Dihalogenated Phenolic Derivates of L-Tyrosine*. Molecules (Basel, Switzerland), 2021. **26**(11).
96. K, R., et al., *Identification of Novel HIV-1 Latency-Reversing Agents from a Library of Marine Natural Products*. Viruses, 2018. **10**(7).
97. SA, R., et al., *Mololipids, a new series of anti-HIV bromotyramine-derived compounds from a sponge of the order verongida*. Journal of natural products, 2000. **63**(4).
98. YB, Z., et al., *Phenolic Compounds from the Flowers of Bombax malabaricum and Their Antioxidant and Antiviral Activities*. Molecules (Basel, Switzerland), 2015. **20**(11).
99. A, E.-D., et al., *Marine Brominated Tyrosine Alkaloids as Promising Inhibitors of SARS-CoV-2*. Molecules (Basel, Switzerland), 2021. **26**(20).
100. CT, L., et al., *Identifying SARS-CoV-2 antiviral compounds by screening for small molecule inhibitors of Nsp3 papain-like protease*. The Biochemical journal, 2021. **478**(13).
101. S, F., et al., *Human immunodeficiency virus type 1 strains R5 and X4 induce different pathogenic effects in hu-PBL-SCID mice, depending on the state of activation/differentiation of human target cells at the time of primary infection*. Journal of virology, 1999. **73**(8).
102. AD, W. and P. AS, *Persistence and emergence of X4 virus in HIV infection*. Mathematical biosciences and engineering : MBE, 2011. **8**(2).
103. Ross, S.A., et al., *Mololipids, a new series of anti-HIV bromotyramine-derived compounds from a sponge of the order verongida*. J Nat Prod, 2000. **63**(4): p. 501-3.
104. Ichiba, T., et al., *Three bromotyrosine derivatives, one terminating in an unprecedented diketocyclopentenylidene enamine*. J. Org. Chem, 1993. **58**(15): p. 4149-4150.
105. Gochfeld, D.J., et al., *Marine natural products as lead anti-HIV agents*. Mini Rev Med Chem, 2003. **3**(5): p. 401-24.
106. ZY, W., et al., *Optimization of the antiviral potency and lipophilicity of halogenated 2,6-diarylpyridinamines as a novel class of HIV-1 NNRTIS*. ChemMedChem, 2014. **9**(7).
107. A, C. and R. E, *From old to new nucleoside reverse transcriptase inhibitors: changes in body fat composition, metabolic parameters and mitochondrial toxicity after the switch from thymidine analogs to tenofovir or abacavir*. Expert opinion on drug safety, 2011. **10**(3).
108. LG, F., et al., *Molecular docking and structure-based drug design strategies*. Molecules (Basel, Switzerland), 2015. **20**(7).

109. L, P. and R. G, *Molecular Docking: Shifting Paradigms in Drug Discovery*. International journal of molecular sciences, 2019. **20**(18).
110. M, B., et al., *Computationally-guided optimization of a docking hit to yield catechol diethers as potent anti-HIV agents*. Journal of medicinal chemistry, 2011. **54**(24).
111. F, A., et al., *HIV nucleoside reverse transcriptase inhibitors*. European journal of medicinal chemistry, 2022. **240**.
112. Ortega, J.T., et al., *The role of the glycosyl moiety of myricetin derivatives in anti-HIV-1 activity in vitro*. AIDS Res Ther, 2017. **14**(1): p. 57.
113. SJ, S., et al., *Structure of the binding site for nonnucleoside inhibitors of the reverse transcriptase of human immunodeficiency virus type 1*. Proceedings of the National Academy of Sciences of the United States of America, 1994. **91**(9).
114. LA, K., et al., *Crystal structure at 3.5 Å resolution of HIV-1 reverse transcriptase complexed with an inhibitor*. Science (New York, N.Y.), 1992. **256**(5065).
115. M, H., Z. M, and D. U, *Inhibition of HIV-1 entry: multiple keys to close the door*. ChemMedChem, 2010. **5**(11).
116. P, G. and M. F, *Recent research results have converted gp120 binders to a therapeutic option for the treatment of HIV-1 infection. A medicinal chemistry point of view*. European journal of medicinal chemistry, 2022. **229**.
117. T, T., et al., *Crystallographic fragment-based drug discovery: use of a brominated fragment library targeting HIV protease*. Chemical biology & drug design, 2014. **83**(2).
118. PS, H., *Biomolecular halogen bonds*. Topics in current chemistry, 2015. **358**.
119. NK, S., d.B. AG, and S. P, *Halogens in Protein-Ligand Binding Mechanism: A Structural Perspective*. Journal of medicinal chemistry, 2019. **62**(21).

SUPPLEMENTARY INFORMATION



Supplementary figure 1. Cell viability of TzM-bl cells **A.** TzM-bl cells treated with AZT. **B.** TzM-bl cells treated DMSO. TzM-bl cells were treated with different concentrations of each compound for 48h. The percentage viability was calculated relative to the no-compound control. Each sample was tested in triplicate in two independent experiments; the results have shown as mean \pm standard deviation.

Compounds (% inhibition)	Concentrations (uM)				
	300	150	75	37	18
TDB-2M	N/A	-51,9	-19,2	-45,5	-57,9
TDB-3M	N/A	-61,9	-18,0	-9,6	-20,5
TDC-2M	47,3*	32,3	37,9	33,0	N/A
TDC-3M	25,9	29,6*	39,7*	20,4	N/A
TODB-2M	N/A	45,8*	37,7	34,1	36,3
TODB-3M	N/A	-9,2	-17,7	-43,3	-26,0
TODC-2M	N/A	61,1*	60,5*	46,4*	38,0*
TODC-3M	59,9*	46,7*	37,6*	54,9*	N/A
YDB-2M	N/A	-45,8	7,0	2,7	26,1
YDB-3M	N/A	N/A	-845,8	-10,2	7,2
YDC-2M	N/A	-2,8	19,1	8,8	-4,1
YDC-3M	N/A	27,5	33,4	42,3*	50,2*
YODB-2M	N/A	-14,9	-88,5	-73,9	-51,1
YODB-3M	N/A	9,3	-9,0	-14,1	-25,1
YODC-2M	N/A	-96,2	26,9	12,2	24,5
YODC-3M	N/A	-1,3	-1,0	-7,7	-19,7

Supplementary table 1. Percentage inhibition of HIV-1 BaL replication of each di-halogenated compound. Each sample was tested in triplicate under two independent experiments. Compounds marked with * showed *p*-values less than 0.0001 when compared to the positive infection control and those marked with N/A have no statistical analysis available.

Concentrations (μM)	150	75	37	18
TDB-2M	2,9	-2,9	15,9	-1,3
TDB-3M	-22,4	-15,7	21,6	2,7
TDC-2M	-72,2	-39,5	-15,4	-4,8
TDC-3M	15,1	8,1	9,6	-110,9
TODB-2M	95,9*	9,9	-4,0	22,2
TODB-3M	-34,0	3,2	-41,1	12,0
TODC-2M	99,6*	62,8	40,6	-18,5
TODC-3M	14,9	26,7	-6,9	-1,3
YDB-2M	-20,7	9,8	-7,0	14,6
YDB-3M	N/A	-19,4	1,8	39,2*
YDC-2M	29,1	22,6	-22,0	15,1
YDC-3M	29,9	31,2	-25,7	41,0*
YODB-2M	-17,0	-20,2	-20,0	-24,6
YODB-3M	13,1	20,3	-10,5	-3,1
YODC-2M	2,5	-2,2	2,3	-0,3
YODC-3M	0,5	-8,6	-5,8	3,2

Supplementary table 2. Percentage inhibition of HIV-1_{MB} (X4 strain) replication of each di-halogenated compound. Each sample was tested in triplicate under two independent experiments. Compounds marked with * showed *p*-values less than 0.001 when compared to the positive infection control and those marked with N/A have no statistical analysis available.

	gp120	RT	gp41	PR	IN	p17	p24
TDB-2M	-4,87 ± 0,19	-6,90 ± 0,00	-3,90 ± 0,00	-9,10 ± 0,00	-4,87 ± 0,38	-5,33 ± 0,09	-5,20 ± 0,00
TDB-3M	-4,50 ± 0,14	-6,23 ± 0,09	-3,90 ± 0,00	-9,20 ± 0,00	-4,43 ± 0,05	-5,10 ± 0,00	-5,20 ± 0,00
TDC-2M	-5,17 ± 0,66	-7,20 ± 0,00	-4,00 ± 0,00	-9,00 ± 0,00	-5,03 ± 0,38	-5,37 ± 0,05	-5,50 ± 0,08
TDC-3M	-4,90 ± 0,00	-6,67 ± 0,05	-4,00 ± 0,00	-9,30 ± 0,00	-4,60 ± 0,00	-5,30 ± 0,00	-5,40 ± 0,00
TODB-2M	-4,77 ± 0,24	-6,40 ± 0,00	-3,83 ± 0,09	-9,07 ± 0,05	-4,47 ± 0,05	-5,33 ± 0,09	-5,30 ± 0,00
TODB-3M	-4,23 ± 0,09	-6,13 ± 0,05	-3,90 ± 0,00	-9,30 ± 0,00	-4,53 ± 0,05	-5,07 ± 0,05	-5,40 ± 0,00
TODC-2M	-4,67 ± 0,05	-6,73 ± 0,09	-4,00 ± 0,00	-9,30 ± 0,00	-4,77 ± 0,31	-5,03 ± 0,05	-5,50 ± 0,08
TODC-3M	-4,83 ± 0,24	-6,10 ± 0,00	-3,90 ± 0,00	-9,37 ± 0,09	-4,50 ± 0,00	-5,07 ± 0,05	-5,60 ± 0,00
YDB-2M	-5,03 ± 0,17	-6,53 ± 0,05	-3,80 ± 0,00	-8,17 ± 0,05	-4,63 ± 0,05	-5,00 ± 0,00	-5,20 ± 0,00
YDB-3M	-4,93 ± 0,45	-6,53 ± 0,05	-3,80 ± 0,00	-8,50 ± 0,00	-4,20 ± 0,08	-4,73 ± 0,05	-5,10 ± 0,00
YDC-2M	-6,10 ± 0,00	-6,97 ± 0,05	-3,97 ± 0,05	-8,30 ± 0,00	-4,67 ± 0,12	-4,80 ± 0,00	-5,20 ± 0,00
YDC-3M	-5,57 ± 0,76	-6,50 ± 0,00	-3,83 ± 0,05	-8,50 ± 0,00	-4,40 ± 0,14	-4,70 ± 0,00	-5,07 ± 0,05
YODB-2M	-4,73 ± 0,17	-6,53 ± 0,05	-3,73 ± 0,05	-8,20 ± 0,00	-4,63 ± 0,09	-4,90 ± 0,00	-5,00 ± 0,00
YODB-3M	-5,17 ± 0,05	-6,20 ± 0,00	-3,53 ± 0,05	-8,40 ± 0,00	-4,30 ± 0,08	-4,70 ± 0,00	-5,10 ± 0,00
YODC-2M	-6,23 ± 0,05	-6,80 ± 0,00	-3,93 ± 0,05	-8,40 ± 0,00	-4,60 ± 0,14	-4,73 ± 0,05	-5,20 ± 0,00
YODC-3M	-5,57 ± 0,90	-6,20 ± 0,00	-3,60 ± 0,00	-8,53 ± 0,05	-4,33 ± 0,05	-4,80 ± 0,00	-5,20 ± 0,00
Fostemsavir	-6,23 ± 0,40	-9,57 ± 0,05	-5,77 ± 0,05	-12,87 ± 0,52	-7,47 ± 0,74	-7,67 ± 0,05	-8,07 ± 0,31
Abacavir	-5,70 ± 0,22	-7,03 ± 0,09	-4,30 ± 0,08	-10,70 ± 0,00	-5,70 ± 0,00	-6,30 ± 0,24	-6,13 ± 0,09
Zidovudine	-6,63 ± 0,66	-7,87 ± 0,05	-4,67 ± 0,05	-10,20 ± 0,00	-5,40 ± 0,00	-5,97 ± 0,33	-6,30 ± 0,00
Efavirenz	-6,00 ± 0,00	-10,10 ± 0,00	-4,90 ± 0,00	-11,60 ± 0,00	-5,30 ± 0,00	-6,40 ± 0,00	-6,10 ± 0,00
Lopinavir	-7,60 ± 0,45	-9,47 ± 0,29	-5,50 ± 0,00	-14,97 ± 0,05	-5,97 ± 0,12	-7,20 ± 0,00	-6,80 ± 0,14
Ritonavir	-5,37 ± 0,39	-8,60 ± 0,00	-4,70 ± 0,22	-13,73 ± 0,05	-5,33 ± 0,12	-6,10 ± 0,36	-6,90 ± 0,43
Dolutegravir	-7,37 ± 0,57	-9,17 ± 0,05	-5,73 ± 0,05	-13,87 ± 0,19	-7,50 ± 0,08	-7,90 ± 0,00	-8,90 ± 0,00
Raltegravir	-7,77 ± 0,78	-8,90 ± 0,00	-5,47 ± 0,05	-13,23 ± 0,12	-7,33 ± 0,24	-7,47 ± 0,12	-7,50 ± 0,14

Supplementary table 3. Binding energies between compounds and viral proteins and study control drugs. Free binding energies were obtained by molecular docking with AutodockVina®. Each interaction was analyzed in triplicate; data represent the mean ± standard deviation. gp120 (glycoprotein 120), RT (Reverse transcriptase), gp41 (glycoprotein 41), PR (protease), IN (integrase), p17 (matrix protein), p24 (capsid protein).

Attachment 1

Review: Natural Products with Inhibitory Activity against Human Immunodeficiency Virus

Type 1. Serna-Arbeláez MS, Florez-Sampedro L, Orozco LP, Ramírez K, Galeano E, Zapata W.

Adv Virol. 2021 May 29; 2021:55520 DOI: 10.1155/2021/5552088. PMID: 34194504; PMCID:

PMC8181102.